IN THE NAME OF
ALLAH
THE MOST
BENIFICIENT
THE MOST MERCIFUL

Mixed Convection Effect in Peristaltic Transport of Nanomaterial

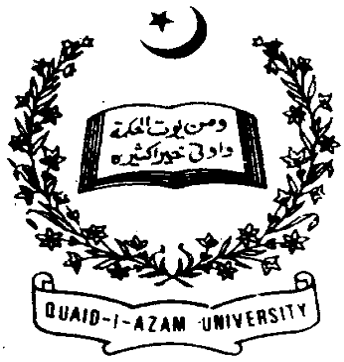

By

Bilal Ahmed

Department of Mathematics
Quaid-I-Azam University
Islamabad, Pakistan
2016

Mixed Convection Effect in Peristaltic Transport of Nanomaterial

By

Bilal Ahmed

Supervised By

Prof. Dr. Tasawar Hayat

Department of Mathematics
Quaid-I-Azam University
Islamabad, Pakistan
2016

Mixed Convection Effect in Peristaltic Transport of Nanomaterial

By

Bilal Ahmed

A DISSERTATION SUBMITTED IN THE PARTIAL FULFILLMENT OF THE REQUIREMENTS FOR THE DEGREE OF THE MASTER OF PHILOSOPHY

IN

MATHEMATICS

Supervised By

Prof. Dr. Tasawar Hayat

Department of Mathematics
Quaid-I-Azam University
Islamabad, Pakistan
2016

Mixed Convection Effect in Peristaltic Transport of Nanomaterial

By

Bilal Ahmed

CERTIFICATE

A DISSERTATION SUBMITTED IN THE PARTIAL FULFILLMENT OF THE REQUIREMENTS FOR THE DEGREE OF THE MASTER OF PHILOSOPHY

We accept this dissertation as conforming to the required standard

1. _____
Prof. Dr. Tasawar Hayat
(Chairman)

2. _____
Prof. Dr. Tasawar Hayat
(Supervisor)

3. _____
Prof. Dr.
(External Examiner)

Department of Mathematics
Quaid-I-Azam University
Islamabad, Pakistan
2016

Dedicated

To

My

Beloved

Mother (Late)

Acknowledgements

Allah Almighty, the merciful, the beneficent, the praise-worthy, has given me the strength to complete this thesis. The sense of He being with me has been the sole reason of my strength throughout the time of hardships. O my Lord I can never thank you for what you have blessed me with. Countless Darood O Salam for the "**Holy Prophet Muhammad**" (peace be upon him), mercy for all the worlds, his off springs and his companions. I offer my humblest gratitude and love to the **Ahle bait** and **Sahaba e Karam**.

I express deepest gratitude to my respected and devoted supervisor **Prof.Dr.Tasawar Hayat**and my co-advisor**Dr. Fahad MunirAbbasi** for their intellectual guidance, constant encouragement, suggestions and inexhaustible inspiration throughout my research work.It is a great honour for me that I am a student of Prof.Dr.Tasawar Hayat.His guidance, creative criticism and kindness made me what I am today.

I am also grateful to all of my respected teachersparticularly Dr.Sohail Nadeem, Dr. Khalid Saifullah, Dr.Masood Khan, Dr. Malik MuhammadYousaf and Dr.Tayyab Kamran for their guidance and support in my M.Phil duration.

What I actually want to say about my family perhaps can't be said. Continuous struggle and untiring hard work of my father **Muhammad Aslam** is the prime reason behind every success I had. I owe my heartiest gratitude for my uncle**Muhammad Iqbal**.I always wish I can be like him, the hardest working man I never seen in my life, a man full of honour and pride. I would love to mention the name of my brothers**Zubair Ahmed, Akif**and**Daoud**. Special thanks to my sisters for their care, love and prayers thatplays a key role in my success. For my Grandmother, Grandfather and Puphuji,I really thanks for their love and countless prayers.

I am especially indebted to all my friends whose presence around me made my life unforgettable and joyful. I am also grateful to my dear friend Rana Anjum Saeed with whom I enjoyed different hues of life. He is like my elder brother. I amthankful to my seniors speciallyFahimbhai (Ustaad…), Taseerbhai (Dr. Sahib), Zubair (IQ), Usman bhai, Jamil bhai, Dr.Rizwan,Dr. Bilal Ashraf andDr.Tayyab (Shah ji) for their continuous support and love.I will never forget the time which I have spent with them.

I wish to express my special thanks to all of my colleagues specially Dr.Farooq (Haji Sahib), Muhammad Waqas, Shahid Farooq, Khursheed, Waleed, Ijaz, Sajjad (Penroz), Azambhai, Arsalan Aziz, Khalil Ch., Tanveer, Gujjar and Mubashir. I am really grateful to my dear friends Fahad Sajjad, Hassan Munir, ManzarJutt and S.Iqbal.

At the end, I would like to pay my gratitude to all others whose names are not mentioned above and have prayed for my success.

BILAL AHMED

30-01-2016

Preface

Peristalsis is well-known mechanism for fluid transport in physiology. In this mechanism sinusoidal waves travel along the walls of tube like organs of human beings propelling the fluid contained within the tube in the direction of their propagation. In physiology the principle of peristalsis is seen in the transport of food through oesophagus, movement of chyme in intestines, urine transport from kidneys to bladder, bile transport in bile duct, transport of spermatozoa, vasomotion of blood vessels and many others. Peristalsis has proven very useful in fluid transport over short distance preventing the fluid from being contaminated. Subject to its utility, such mechanism has been adopted by the engineers in designing several industrial appliances including roller and fingers pumps and peristaltic pumps in heart lung and dialysis machines. Latest hose pumps of several kinds operate through the principle of peristalsis. Peristaltic type flow is readily being used in the nuclear industry for the transport of corrosive fluids. Latham [1] initially presented the study of peristaltic flow of a viscous fluid. Jaffrin and Shapiro [2] have provided survey of early literature on the peristaltic transport of fluids. Some other fundamental studies, on peristalsis include Fung and Yih [3] and Srivastava [4]. Subject to such wide occurrence of peristalsis in physiology and industry, many theoretical investigations have been carried out in different flow configuration [5,6].

Heat transfer plays a key role in countless industrial and engineering processes as energy input in several complex systems or in a form of energy output produced by the system itself which needs to be removed by cooling systems. Usually the heat transfer takes place through flow of appropriate heat transfer fluids i.e. air, water, mineral oil, etc. Low thermal conductivity of such fluids proved to be one major constraint in their use as heat transfer fluids. It is well established now that the addition of nanometer sized particles enhances the thermal conductivity of conventional fluids. The mixture obtained by adding nanoparticles to the base fluids is known as nanofluid, a term introduced by Choi [7]. Commonly used nanoparticles are metallic oxides (CuO,TiO_2,Al_2O_3,ZnO), metals (Cu,Ag and Au), nitride/carbide ceramics (AIN,SiN,SiC,Ti), single/multi-walled CNTs and composite materials such as alloyed nanoparticles Al_7OCu_3 [8-10]. Water, ethylene glycol and oil are generally used as base fluids. Nanofluids find extensive applications in modern heating and cooling systems, in solar collector, biomedical engineering, detection of radiation, modern drug delivery system etc. The wide utility of nanofluids is the

reason for growing interest in nanofluid mechanics by the researchers of modern era. Expressions for the effective density and viscosity of the nanofluids were computed by Xuan and Li [11]. Brinkman [12] model for the effective viscosity of the two phase flow was found to be in good agreement with the experimental results of Xuan and Li.[11]. Some studies using the two phase flow model of nanofluids can be seen through refs. [13-17].

It is now well admitted fact that all the tubular organs facilitating fluid flow in the human body are internally lubricated with mucus and secretion layers. These layers in turn prevent the fluid from sticking to the walls. In such cases the no-slip condition between the fluid and solid boundary is not valid. With such motivation some authors investigated the peristaltic transport of ordinary fluids with slip effects [18-19]. Mixed convective flows have received numerous attention from the researchers the word over due to their wide industrial and engineering applications. Convection is seen in the ocean currents, sea-wind formation, formation of micro-structures during the cooling of molten metals, solar ponds and in fluid flows around heat dissipation fins. Convection in channels plays a vital role in heat exchangers, removal of nuclear waste and in modern cooling/heating systems. Hayat et al. [20-21] have seen the influence of mixed convection on the peristaltic flow.

First chapter is concerned with the basic definitions and equations which are relevant to the subsequent chapters. Chapter two describes the copper-water nanofluid to discuss the peristaltic flow in a symmetric channel with slip conditions. This study extends the two-phase flow model of peristaltic motion with temperature jump conditions in an inclined channel.

Chapter three investigates the mixed convection peristalsis of the single wall carbon nanotubes (SWCNT) through an inclined channel. The velocity slip and temperature jump conditions are also taken into account. It is noted that none of the above mentioned studies investigated the peristalsis of the Single Walled Carbon Nanotubes (SWCNTs) yet. This study aims to fill this void. Three different thermal conductivity models, namely the Maxwell [22], the Hamilton-Crosser [23] and the Xue [24] are used for the analysis. Series solutions for the resulting nonlinear system are obtained and analyzed. Comparison between the copper nanaoparticles and the SWCNT case is also provided. Influences of various parameters of interest are analyzed through graphical and tabular representations.

Contents

Chapter 1

Introduction

The basic objective of this chapter is to present some fundamental concepts and governing equations that will facilitate the understanding of the subsequent chapters.

1.1 Basic definitions

1.1.1 Fluid

Fluid is described as a material deforming continuously under the action of applied shear stress of any magnitude. Major difference between solids and fluids is that the solids do not deform continuously whereas in the fluids the deformation continues indefinitely.

1.1.2 Fluid mechanics

It is a branch in which the fluids at rest or in motion can be described as follows:

Fluid dynamics

The branch of engineering that studies the behavior of fluids in motion is known as fluid dynamics.

Fluid statics

It is the study of the behavior of fluids at rest.

1.1.3 Density of a fluid

Density is the property of a material (fluid) that describes the mass of a unit volume of the substance at a specific temperature and pressure. At a point the density can be expressed as follows:

$$\rho = \lim_{\delta->0}(\frac{\delta m}{\delta v}). \tag{1.1}$$

In the above equation δm denotes the mass element, δv is the volume element enclosing the point under consideration and ρ indicates the fluid density. The SI unit of density is kg/m^3 with dimension $\left[\frac{M}{L^3}\right]$.

1.1.4 Viscosity of a fluid

Viscosity is defined as the property of fluid to resist the deformation. Physically it is described as the ratio of shear stress and shear strain. The mathematical relationship for viscosity is

$$Viscosity(\mu) = \frac{\text{shear stress}}{\text{rate of shear strain}}.$$

Viscosity is significant in both experimental and theoretical analysis of fluid. It is further categorized into absolute, kinematic or dynamic viscosity. The SI unit of viscosity is $kg/m.s$ with dimensions $\left[\frac{M}{LT}\right]$.

1.1.5 Kinematics viscosity

The ratio of absolute viscosity (dynamic viscosity) of fluid to the fluid density. Mathematically it is given as follows:

$$\text{Kinematic viscosity } (\nu) = \frac{\mu}{\rho}.$$

Its SI unit is m^2/s with dimensions is $\left[\frac{L^2}{T}\right]$.

1.1.6 Pressure

The magnitude of force perpendicular to the surface area is called pressure. Mathematically it is given through the following relation:

$$\text{Pressure} = \frac{\text{Magnitude of applied force}}{\text{area}} = \frac{F}{A}.$$

1.1.7 Flow

The fluid tends to deform under the action of applied stress. When such deformation continues indefinitely then this phenomena is called flow.

Steady flow

If all the physical properties of a fluid are independent of time then such flow is named as steady flow. If ζ is any fluid property then for a steady flow one must have

$$\frac{\partial \zeta}{\partial t} = 0. \tag{1.2}$$

Unsteady flow

The flow in which the physical properties of the fluid vary with time is known as unsteady flow.

Compressible flow

If the density of fluid varies then it is called compressible flow. In generally flow of gases are considered as compressible flows.

Incompressible flow

The flow in which density of the fluid remains constant is called incompressible flow. Generally flow of liquid are characterized as incompressible flows.

1.1.8 Stream function

It is a function, which illustrates the flow pattern of fluid that represents discharge per unit thickness. It characterizes the flow field in terms of mass flow rate for compressible fluid and volume flow rate for an incompressible fluid. For steady two dimensional flow it can be defined

as

$$V = \nabla \times \boldsymbol{\psi}, \tag{1.3}$$

here $V = (u, v, 0)$ so according to above equation $\boldsymbol{\psi} = (0, 0, \psi)$. The stream function helps us to study the flow behavior graphically by drawing the streamlines (ψ =constant). Velocity components in terms of stream function are defined as

$$u = \frac{\partial \psi}{\partial y}, v = -\frac{\partial \psi}{\partial x}. \tag{1.4}$$

1.1.9 Ideal and real fluids

Fluid which have negligible viscosity are called ideal fluids. Ideal fluids do not exist in nature, but in many applications gases are treated as ideal fluids. Further the fluids with non-zero viscosity are called real fluids. All existing fluids are real fluid. Real fluids are further classified into Newtonian and Non-Newtonian fluids.

1.1.10 Newtonian fluids

If the shear stress is directly and linearly proportional to the rate of strain then such fluids are called the Newtonian fluids. Mathematically for Newtonian fluids:

$$\tau_{yx} \propto \frac{du}{dy}$$

or

$$\tau_{yx} = \mu \frac{du}{dy}. \tag{1.5}$$

In the above expression τ_{yx} denotes shear stress, μ dynamic viscosity and du/dy the rate of strain for one-dimensional flow. In this case, viscosity depends on pressure and temperature. For constant viscosity and incompressible flow shear stress can be generalized in Cartesian coordinate system as follows:

$$\tau_{ij} = \mu(\frac{\partial u_i}{\partial y_j} + \frac{\partial u_j}{\partial y_i}) \tag{1.6}$$

In above expression

τ_{ij} is the shear stress on the i^{th} face of a fluid element in the j^{th} direction

u_i is the velocity in the i^{th} direction

y_j is the j^{th} direction coordinates

Common examples of Newtonian fluids are water and gasoline. In this dissertation, the considered flows will be analyzed for the viscous fluid situation.

1.1.11 Types of forces

Surface forces

Any particular force that acts through direct contact with the fluid's surface is called surface force. For example, pressure and stresses.

Body forces

If the force does not have physical contact with the object surface, but acts throughout the volume of the fluid then such force is named as body force. Magnetic force and force of gravity are the examples of body forces.

1.1.12 Volume flow rate

It is the volume of fluid which passes through a section of a pipe or channel in unit time. It is usually represented by the symbol Q. If 'A' is the given area and V is the fluid's velocity, making an angle θ with the perpendicular to A, then the volume flow rate is given as:

$$Q = AVcos\theta.$$

If the flow is perpendicular to the area A then $\theta = 0$ and thus the volume flow rate is

$$Q = AV.$$

1.1.13 No-slip condition

During the fluid flow molecules tend to stick with the solid boundary and move with the velocity of the wall. This mechanism is known as no-slip condition.

1.1.14 Slip condition

In many engineering applications and biological phenomena the no-slip condition is not applicable, so Navier proposed the relative velocity between the fluid and wall which is known as slip condition. Relative velocity between the fluid and solid boundary is directly proportional to the shear stress at the boundary. Mathematically we have

$$u_f - u_w \propto \tau_{xy},$$

or

$$u_f - u_w = \pm \frac{\beta}{\mu} \tau_{xy}. \tag{1.7}$$

Here u_f denotes the velocity of fluid, u_w the velocity of wall, β the slip parameter, $+ve$ and $-ve$ signs show the condition at upper and lower walls respectively. Note that the no-slip condition can be retained by substituting $\beta = 0$.

1.2 Peristalsis

The word peristalsis is derived from a Greek word "Peristaltikos" which means pumping and clasping. It is the mechanism of mixing and transporting the fluid by the contraction or expansion of channel wall through the progressive waves. Transport mechanism taking use of peristalsis is named as peristaltic transport.

1.2.1 Occurrence of peristalsis in physiology

Peristalsis being a major mechanism of fluid transport holds much significance in physiology. Transport of food bolus through bile duct, sperm/ egg movement through male/ female reproductive tract, urine transport from kidneys to the bladder is carried out using the mechanism of peristalsis. In this mechanism waves of area contraction and relaxation travel along the channel walls. These waves in turn propel the fluid contained within the channel.

1.2.2 Pumping

A pump transfers liquid from one location to another under the certain conditions and this mechanical mechanism is called pumping. It is further classified as below:

Positive and negative pumping

The positive and negative pumping is based on the dimensional mean flow rate η. If η is positive then pumping is also positive or vice versa.

Peristaltic pumping

Peristaltic pumping behavior appears for the positive flow rate and adverse pressure gradient, i.e. $\Delta P_\lambda > 0$ and $\eta > 0$.

Free pumping

In this case, flow rate is positive and pressure gradient is neither positive nor negative. In this momentous point $\Delta P_\lambda = 0$.

Co-pumping or augmented pumping

In this case pumping is positive and pressure gradient is favorable i.e. $\Delta P_\lambda < 0$ and $\eta > 0$.

1.2.3 Bolus

During the fluid flow some volume of the fluid bounded by closed streamlines in the wave frame which is called bolus.

1.2.4 Trapping

In the fluid flow streamlines trap some volume of fluid and the peristaltic wave move the trapped volume of fluid with the wave speed that is known as trapping phenomena.

1.3 Nanomaterials and Nanofluids

1.3.1 Nanomaterial

Natural or manufactured materials which have size upto $1 - 100$ nanometer with at least one-dimension are called nanomaterials. They have unique physical, electrical and mechanical properties. Nanomaterials occur naturally in the different forms like viruses, foraminifera (mainly chalk), natural colloids (milk, blood), horny materials (skin, claws, horns, hair), paper,

cotton and clay e.t.c. There are different synthesized nanomaterials such as metallic oxides (CuO, TiO_2, Al_2O_3, ZnO), metals (Cu, Ag and Au), nitride/Carbide ceramics (AIN, SiN, SiC, TiC), Single/multi-walled Carbon nanotubes and composite materials such as alloyed nanoparticles Al_7OCu_3O.

1.3.2 Nanofluid

The mixture of nanometer-sized particles suspended in the base fluid is called nanofluid. Nanoparticle are colloidally suspended in the base fluid. Nanofluids enhance the thermo-physical properties and heat transfer performance in many biological and industrial applications. Nanofluids are widely used in cooling of electronics, cooling of heat exchanging devices and improve their efficiency, automobile industry, in the solar collectors, in nuclear reactors and modern drug delivery systems. Different types of fluids are as base fluids e.g. water, ethylene glycol, oil e.t.c.

1.3.3 Thermal conductivity models of nanofluids

The suspension of solid nanoparticles enhances the thermal conductivity of liquid fluid. Some of the available models that predict the thermal conductivity of a two phase flow (i.e fluid-solid phases) are given below:

Maxwell's model

Maxewell predicted the effective thermal conductivity (K_{eff}) model [22] for spherical solid materials suspended in fluid and is given as follows:

$$\frac{K_{eff}}{K_f} = \frac{K_p + 2K_f - 2\phi(K_f - K_p)}{K_p + 2K_f + \phi(K_f - K_p)}. \tag{1.8}$$

In the above equations K_f denotes the thermal conductivity of the base fluid, K_p the thermal conductivity of nanomaterials and ϕ the volume fraction for the nanomaterial.

Hamilton-Crosser's model

Hamilton-Crosser's (H-C) generalized the Maxwell's model for the non-spherical particles.

The H-C's model [23] of thermal conductivity of nanofluids is

$$\frac{K_{eff}}{K_f} = \frac{K_p + (n-1)K_f - (n-1)\phi(K_f - K_p)}{K_p + (n-1)K_f + \phi(K_f - K_p)}. \tag{1.9}$$

Here "n" represents the structure formate of nanoparticles given by $3/\Psi$ and Ψ is the sphericity of the nanomaterial that depends on their shape. Here $\Psi = 1$ or $n = 3$ for the spherical nanomaterial and the H-C's model is reduced into Maxewell's model. Further $\Psi = 1/2$ or $n = 6$ is for the cylindrical nanomaterial. For SWCNTs we use $n = 6$ in the H-C's model.

Xue's model

Xue proposed a new model [24] to calculate the thermal conductivity of nanotubes. Xue's model is given as:

$$\frac{K_{eff}}{K_f} = \frac{1 - \phi + 2\phi\frac{K_{CNT}}{K_{CNT}\text{-}K_f}[\ln\frac{K_{CNT}+K_f}{2K_f}]}{1 - \phi + 2\phi\frac{K_f}{K_{CNT}\text{-}K_f}[\ln\frac{K_{CNT}+K_f}{2K_f}]}, \tag{1.10}$$

here K_{CNT} represents the thermal conductivity of carbon nanotubes.

1.4 Basics of heat transfer

1.4.1 Heat

Heat is the summation of kinetic energy of the system. This form of energy plays a significant role in the transfer of energy from one place to another due to the change in temperature.

1.4.2 Heat transfer

Heat transfer is the phenomena by which heat flows within the system due to the variation in temperature. Heat transfers from a hot to cold region. Heat transfer rate depends on the temperature gradient, and it continuously flows until temperature gradient approaches zero.

1.4.3 Modes of heat transfer

There are three mechanisms through which heat is transferred from one place to another namely conduction, convection and radiation.

1.4.4 Specific heat

The amount of heat energy required to enhance the temperature by one degree of one kg substance is known as the specific heat of that substance.

1.4.5 Thermal conductivity

The property of a material to transmit or to conduct heat energy is known as thermal conductivity. It is denoted by k. A substance that has high thermal conductivity is a good conductor and is used in heat sink applications and lower thermal conductivity materials are used as heat insulators. The thermal conductivity of substance may depend on the temperature. The unit of thermal conductivity is $kg.m/s^3.K$ with dimension $\left[\frac{ML}{T^3\theta}\right]$.

1.4.6 Viscous dissipation

When the viscous fluid flows kinetic energy of the fluid transforms into internal energy due to the viscous effects. This phenomena is named as viscous dissipation.

1.5 Dimensionless numbers

Sometimes equations are complicated in the fluid mechanics so we use dimensionless numbers and parameters to simplify the given flow problem. The dimensionless number used in this dissertation are defined below:

1.5.1 Reynolds number

It is the ratio of inertial forces to the viscous forces of fluid. Mathematically

$$Re = \frac{\rho v L}{\mu},$$

here ρ is the density, v the flow velocity of object, L the characteristic length and μ the dynamic viscosity of fluid. When Reynold's number is high viscous effects are dominant and fluid is turbulent and for laminar flow Reynolds number is small.

1.5.2 Wave number

The ratio of the channel width to the wavelength is known as wave number. Mathematically it is represented as

$$\delta = \frac{d}{\lambda},$$

here d is the half channel width and λ is the wavelength.

1.5.3 Prandtl number

It describes the ratio of momentum diffusivity (kinetic energy) to the thermal diffusivity. Mathematically it is expressed as:

$$Pr = \frac{\mu C_p}{K},$$

here C_p denotes specific heat and K the thermal conductivity of fluid.

1.5.4 Eckert number

The ratio of kinetic energy and enthalpy is known as Eckert number. This parameter enters in flow modality due to viscous effects. It is defined as

$$E = \frac{v^2}{C_p \Delta T},$$

here ΔT the temperature difference between fluid and boundary.

1.5.5 Brinkman number

It is the ratio of viscous dissipation to the heat transfer rate. It can be described by the product of Prandtl number and Eckert numbers as:

$$Br = PrE.$$

1.5.6 Grashoff number

The ratio of buoyancy forces to the viscous forces that are acting on fluid volume is named as Grashoff number. It is defined as

$$Gr = \frac{g\beta\Delta T L^3}{\upsilon^2},$$

here β the thermal expansion coefficient, g the acceleration due to gravity and υ the kinematic viscosity of fluid.

1.6 Basic governing equations

1.6.1 Continuity equation

The conservation law of mass leads to the fact that mass of a closed system remains constant, regardless of the processes acting inside the system. This principle can be applied to a moving fluid and its mathematical formulation yields the continuity equation. With no source or sink in the control volume, the continuity equation is given as

$$\frac{\partial \rho}{\partial t} + \frac{\partial(\rho u)}{\partial x} + \frac{\partial(\rho v)}{\partial y} + \frac{\partial(\rho w)}{\partial z} = 0, \tag{1.11}$$

where u,v and w designate the velocity components in x,y and z directions respectively. Eq. (1.11) can be presented as follows

$$\frac{\partial \rho}{\partial t} + \nabla.\rho V = 0. \tag{1.12}$$

For incompressible fluid, the continuity equation takes the following form

$$\nabla.V = 0,$$

or

$$\operatorname{div} V = 0. \tag{1.13}$$

1.6.2 Equation of motion

The vectorial form of equation of motion is given as:

$$\rho\frac{dV}{dt} = \operatorname{div} T + \rho b, \tag{1.14}$$

where $\mathbf{T}$ is the Cauchy stress tensor, ρb is the body force and d/dt is the material derivative given as

$$\frac{d}{dt} = \frac{\partial}{\partial t} + u\frac{\partial}{\partial x} + v\frac{\partial}{\partial y} + w\frac{\partial}{\partial z},$$

or

$$\frac{d}{dt} = \frac{\partial}{\partial t} + V.\nabla. \tag{1.15}$$

The Cauchy stress tensor $\mathbf{T}$ is given as:

$$\mathbf{T} = \begin{bmatrix} \sigma_{xx} & \tau_{xy} & \tau_{xz} \\ \tau_{yx} & \sigma_{yy} & \tau_{yz} \\ \tau_{zx} & \tau_{zy} & \sigma_{zz} \end{bmatrix} \tag{1.16}$$

in which σ_{xx}, σ_{yy} and σ_{zz} denote the normal stresses and τ_{ij} $(ij \neq 0)$ are the shear stresses.

1.6.3 Energy equation

The conservation law of the energy describes that the increase in the internal energy of a thermodynamic system is equal to the amount of energy gained (lost) by the system. The general form of energy equation is

$$\rho\zeta\frac{dT}{dt} = \bar{\mathbf{T}}.(\nabla V) + \nabla.(k\nabla T). \tag{1.17}$$

In which ζ is a specific heat at constant volume and k is the thermal conductivity of fluid.

Chapter 2

Mixed convective peristalsis of nanofluid in presence of partial slip

2.1 Introduction

The objective of this chapter is to explore the features of peristalsis of nanofluid in an inclined channel. Effects of slip conditions due to velocity and temperature are addressed. Lubrication approach has been employed for the present analysis. Series solutions are obtained by using perturbation technique. These series solutions are used to sketch the graphs of velocity, streamlines, pressure gradient, pressure rise per wavelength, temperature and heat transfer rate at the boundary. Further, these plots are also physically analyzed.

2.2 Definition of the problem

We investigate the two-dimensional flow of nanomaterials in an inclined channel of uniform width $2d$. An incompressible nanofluid is composed of nanomaterial and water. Both of these materials are in thermal equilibrium. We select $\overline{X} - axis$ is parallel to the channel wall and $\bar{Y} - axis$ is transverse direction to the $\overline{X} - axis$. The peristalsis here is in view of propagating wave along the channel walls. The waves have amplitude a_1, wavelength λ and constant speed

c. The wall shape for the peristaltic phenomena is represented as:

$$\begin{aligned} +\overline{H}(\bar{X},\bar{t}) &= +d + a_1 cos(\frac{2\pi}{\lambda}(\bar{X} - c\bar{t})), \\ -\overline{H}(\bar{X},\bar{t}) &= -d - a_1 cos(\frac{2\pi}{\lambda}(\bar{X} - c\bar{t})). \end{aligned} \tag{2.1}$$

Here t is the time and $+ve$ and $-ve$ signs indicate the upper and lower walls of the channel.

2.3 Problem formulation

The velocity field for the present flow configuration in the laboratory frame is $\mathbf{V} = [\bar{U}(\bar{X},\bar{Y},\bar{t}), \bar{V}(X,\bar{Y},\bar{t}), 0]$. Here $\bar{U}$ and $\bar{V}$ denote the velocities parallel to the $\bar{X} - axis$ and $\bar{Y} - axis$. Cauchy stress tensor for viscous incompressible fluid is

$$\bar{\mathbf{T}} = -\bar{P}\bar{\mathbf{I}} + \bar{\mu}\bar{\mathbf{A}}_1, \tag{2.2}$$

in which I represent the identity tensor, $\bar{P}(X,Y,t)$ the pressure, $\bar{\mu}$ the dynamic viscosity and Rivlin Ericksen tensor $\bar{\mathbf{A}}_1$ is

$$\bar{\mathbf{A}}_1 = (\nabla V) + (\nabla V)^t, \tag{2.3}$$

$$\nabla V = \begin{bmatrix} \frac{\partial \bar{U}}{\partial \bar{X}} & \frac{\partial \bar{U}}{\partial \bar{Y}} & 0 \\ \frac{\partial \bar{V}}{\partial \bar{X}} & \frac{\partial \bar{V}}{\partial \bar{Y}} & 0 \\ 0 & 0 & 0 \end{bmatrix},$$

$$(\nabla V)^t = \begin{bmatrix} \frac{\partial \bar{U}}{\partial \bar{X}} & \frac{\partial \bar{V}}{\partial \bar{X}} & 0 \\ \frac{\partial \bar{U}}{\partial \bar{Y}} & \frac{\partial \bar{V}}{\partial \bar{Y}} & 0 \\ 0 & 0 & 0 \end{bmatrix},$$

the superscript "t" represents the transpose of the matrix and $\bar{\mathbf{A}}_1$ is

$$\bar{\mathbf{A}}_1 = \begin{bmatrix} 2\frac{\partial \bar{U}}{\partial \bar{X}} & \frac{\partial \bar{V}}{\partial \bar{X}} + \frac{\partial \bar{U}}{\partial \bar{Y}} & 0 \\ \frac{\partial \bar{U}}{\partial \bar{Y}} + \frac{\partial \bar{V}}{\partial \bar{X}} & 2\frac{\partial \bar{V}}{\partial \bar{Y}} & 0 \\ 0 & 0 & 0 \end{bmatrix}.$$

The relevant equations are

$$div\bar{\mathbf{V}} = 0, \tag{2.4}$$

$$\rho\frac{d\bar{\mathbf{V}}}{dt} = \text{div}\,\bar{\mathbf{T}} + \rho b, \tag{2.5}$$

$$\rho c\frac{dT}{dt} = \bar{\mathbf{T}}.(\nabla V) + \nabla.(k\nabla T). \tag{2.6}$$

Here ρ is the fluid density, k the thermal conductivity and b the body force. The channel walls have temperature T_0. Analysis is carried out in the presence of heat source/ sink parameter Φ and mixed convection. The equations of motion, momentum and energy are

$$\frac{\partial\bar{U}}{\partial\bar{X}} + \frac{\partial\bar{V}}{\partial\bar{Y}} = 0, \tag{2.7}$$

$$\begin{aligned}\rho_{nf}(\frac{\partial}{\partial\bar{t}} + \bar{U}\frac{\partial}{\partial\bar{X}} + \bar{V}\frac{\partial}{\partial\bar{Y}})\bar{U} &= -\frac{\partial\bar{P}}{\partial\bar{X}} + \mu_{eff}(\frac{\partial^2\bar{U}}{\partial\bar{X}^2} + \frac{\partial^2\bar{U}}{\partial\bar{Y}^2}) \\ &\quad +g(\rho\beta)_{nf}(T - T_0)sin\alpha,\end{aligned} \tag{2.8}$$

$$\begin{aligned}\rho_{nf}(\frac{\partial}{\partial\bar{t}} + \bar{U}\frac{\partial}{\partial\bar{X}} + \bar{V}\frac{\partial}{\partial\bar{Y}})\bar{V} &= -\frac{\partial\bar{P}}{\partial\bar{Y}} + \mu_{eff}(\frac{\partial^2\bar{V}}{\partial\bar{X}^2} + \frac{\partial^2\bar{V}}{\partial\bar{Y}^2}) \\ &\quad -g(\rho\beta)_{nf}(T - T_0)cos\alpha,\end{aligned} \tag{2.9}$$

$$\begin{aligned}(\rho C)_{nf}(\frac{\partial}{\partial\bar{t}} + \bar{U}\frac{\partial}{\partial\bar{X}} + \bar{V}\frac{\partial}{\partial\bar{Y}})\bar{T} = K_{eff}(\frac{\partial^2\bar{T}}{\partial\bar{X}^2} + \frac{\partial^2\bar{T}}{\partial\bar{Y}^2}) + \Phi \\ +\mu_{eff}[2((\frac{\partial\bar{U}}{\partial\bar{X}})^2 + (\frac{\partial\bar{V}}{\partial\bar{Y}})^2) + (\frac{\partial\bar{U}}{\partial\bar{Y}} + \frac{\partial\bar{V}}{\partial\bar{X}})^2].\end{aligned} \tag{2.10}$$

Two phase flow model's of effective viscosity μ_{eff}, effective density ρ_{nf}, effective thermal conductivityK_{eff} , effective thermal expansion coefficient $(\rho\beta)_{nf}$ and effective heat capacity $(\rho C)_{nf}$ of nanofluid are given as follows:

$$\begin{aligned}\mu_{eff} &= \frac{\mu_f}{(1-\phi)^{2.5}}, \\ \rho_{nf} &= (1-\phi)\rho_f + \phi\rho_p, \\ (\rho C)_{nf} &= (1-\phi)(C\rho)_f + \phi(C\rho)_p, \\ (\rho\beta)_{nf} &= (1-\phi)\rho_f\beta_f + \phi\rho_p\beta_p, \\ \frac{K_{eff}}{K_f} &= \frac{K_p + 2K_f - 2\phi(K_f - K_p)}{K_p + 2K_f + \phi(K_f - K_p)}.\end{aligned} \tag{2.11}$$

Here $\mu_f,\ \rho_f,\ \rho_p,\ C_f,\ C_p,\ \beta_f,\ \beta_p,\ K_f,\ K_p$ and ϕ represent the viscosity of fluid, density of water, the density of nanomaterials, specific heat of water, specific heat of nanomaterials, thermal expansion coefficient of water, thermal expansion coefficient of nanomaterials, thermal conductivity of water, thermal conductivity of nanomaterials and volume fraction of nanomaterials respectively.

2.4 Governing equations in the wave frame

For the transformation of the system of equations from the laboratory frame of to wave frame of reference the following relations are used:

$$\bar{x} = \bar{X} - c\bar{t}, \bar{y} = \bar{Y}, \bar{u} = \bar{U} - c, \bar{v} = \bar{V}, \bar{p}(\bar{x}, \bar{y}) = \bar{P}(\bar{X}, \bar{Y}, \bar{t}). \tag{2.12}$$

In the above expression $\bar{p}(\bar{x}, \bar{y})$ is the pressure, $\bar{u}(\bar{x}, \bar{y})$ and $\bar{v}(\bar{x}, \bar{y})$ are the longitudinal and transverse components of velocity in the wave frame respectively. Following Eq. (2.12) we obtain:

$$\frac{\partial \bar{u}}{\partial \bar{x}} + \frac{\partial \bar{v}}{\partial \bar{y}} = 0, \tag{2.13}$$

$$\begin{aligned}((1-\phi)\rho_f + \phi\rho_p)((\bar{u}+c)\frac{\partial}{\partial \bar{x}} + \bar{v}\frac{\partial}{\partial \bar{y}})(\bar{u}+c) = -\frac{\partial \bar{p}}{\partial \bar{x}} + \frac{\mu_f}{(1-\phi)^{2.5}}(\frac{\partial^2 \bar{u}}{\partial \bar{x}^2} + \frac{\partial^2 \bar{u}}{\partial \bar{y}^2}) \\ +g((1-\phi)\rho_f\beta_f + \phi\rho_p\beta_p)(T-T_0)sin\alpha,\end{aligned} \tag{2.14}$$

$$\begin{aligned}((1-\phi)\rho_f + \phi\rho_p)((\bar{u}+c)\frac{\partial}{\partial \bar{x}} + \bar{v}\frac{\partial}{\partial \bar{y}})\bar{v} = -\frac{\partial \bar{p}}{\partial \bar{y}} + \frac{\mu_f}{(1-\phi)^{2.5}}(\frac{\partial^2 \bar{v}}{\partial \bar{x}^2} + \frac{\partial^2 \bar{v}}{\partial \bar{y}^2}) \\ +g((1-\phi)\rho_f\beta_f + \phi\rho_p\beta_p)(T-T_0)cos\alpha,\end{aligned} \tag{2.15}$$

$$\begin{aligned}((1-\phi)(C\rho)_f + \phi(C\rho)_p)((\bar{u}+c)\frac{\partial}{\partial \bar{x}} + \bar{v}\frac{\partial}{\partial \bar{y}})T = K_{eff}(\frac{\partial^2 T}{\partial \bar{x}^2} + \frac{\partial^2 T}{\partial \bar{y}^2}) \\ +\Phi + \frac{\mu_f}{(1-\phi)^{2.5}}[2((\frac{\partial \bar{u}}{\partial \bar{x}})^2 + (\frac{\partial \bar{v}}{\partial \bar{y}})^2) + (\frac{\partial \bar{u}}{\partial \bar{y}} + \frac{\partial \bar{v}}{\partial \bar{x}})^2].\end{aligned} \tag{2.16}$$

2.5 Non-dimensionalization of the problem

For the present flow phenomena the dimensionless quantities are as follows:

$$\begin{gathered} x=\frac{\overline{x}}{\lambda}, y=\frac{\overline{y}}{d}, u=\frac{\overline{u}}{c}, v=\frac{\overline{v}}{c\delta}, \delta=\frac{d}{\lambda}, h=\frac{\overline{H}}{d}, a=\frac{a_1}{d}, p=\frac{d^2\overline{p}}{c\lambda\mu_f}, \\ \upsilon=\frac{\mu_f}{\rho_f}, Re=\frac{\rho_f\ cd}{\mu_f}, t=\frac{ct}{\lambda}, E=\frac{c^2}{C_fT_0}, pr=\frac{\mu_fC_f}{K_f}, Gr=\frac{\rho_fg\beta_fT_0d^2}{\mu_fc}, \\ \theta=\frac{T-T_0}{T_0}, Br=PrE, \varepsilon=\frac{d^2\Phi}{T_0K_f}, u=\frac{\partial\psi}{\partial y}, v=-\frac{\partial\psi}{\partial x}. \end{gathered} \tag{2.17}$$

Using above variables and long wavelength and low Reynold number consideration are obtains

$$\frac{\partial p}{\partial x}=\frac{1}{(1-\phi)^{2.5}}\frac{\partial^3\psi}{\partial y^3}+Grsin\alpha\{1-\phi+\phi(\frac{(\rho\beta)_p}{(\rho\beta)_f})\}\theta, \tag{2.18}$$

$$p_y=0, \tag{2.19}$$

$$[\frac{K_p+2K_f-2\phi(K_f-K_p)}{K_p+2K_f+\phi(K_f-K_p)}]\frac{\partial^2\theta}{\partial y^2}+\frac{Br}{(1-\phi)^{2.5}}(\frac{\partial^2\psi}{\partial y^2})^2+\varepsilon=0, \tag{2.20}$$

where incompressibility condition is automatically satisfied. Cross differentiation of Eq. (2.18) and Eq. (2.19) yields:

$$0=\frac{1}{(1-\phi)^{2.5}}\frac{\partial^4\psi}{\partial y^4}+Grsin\alpha\{1-\phi+\phi(\frac{(\rho\beta)_p}{(\rho\beta)_f})\}\frac{\partial\theta}{\partial y}.$$

Here δ, α, p, υ, Re, E, Pr, Gr, θ, Br, ϵ and ψ denote the wave number, inclination angle, pressure, kinematic viscosity, Reynolds number, Eckert number, Prandtl number, Grashoff number, dimensionless temperature, Brinkman number, dimensionless heat generation/ absorption parameter and stream function respectively.

2.6 Volume flow rate and boundary conditions

The dimensionless mean flow rate for symmetric channel in laboratory $\eta(=\frac{\bar{Q}}{cd})$ and moving frames $F(=\frac{\bar{q}}{cd})$ are related by

$$\eta=F+1, \tag{2.21}$$

in which

$$F = \int_0^h \frac{\partial \psi}{\partial y} dy. \tag{2.22}$$

For the existing flow behavior the boundary conditions along with the velocity slip and temperature jump conditions [19] are given as:

$$\begin{gathered} \psi = 0, \psi_{yy} = 0, \theta_y = 0, \text{ at } y = 0, \\ \psi = F, \frac{\partial \psi}{\partial y} + \frac{\beta}{(1-\phi)^{2.5}} \frac{\partial^2 \psi}{\partial y^2} = -1, \theta + \gamma \frac{\partial \theta}{\partial y} = 0, \text{ at } y = h, \end{gathered} \tag{2.23}$$

where $h = 1 + a\ cos(2\pi x)$ is the dimensionless wall shape. Pressure rise per wavelength (ΔP_λ) is defined as:

$$\Delta P_\lambda = \int_0^1 (\frac{dp}{dx}) dx. \tag{2.24}$$

2.7 Series solutions

We expand the flow quantities in the increasing powers of "Br", to obtain the solutions of the Eqs. (2.18) – (2.20), subjected to the boundary conditions (2.23) as follows:

$$\begin{gathered} \psi = \psi_0 + Br\psi_1 + O(Br^2) + ... \\ \theta = \theta_0 + Br\theta_1 + O(Br^2) + ... \\ p = p_0 + Brp_1 + O(Br^2) + ... \\ F = f_0 + Brf_1 + O(Br^2) + ... \end{gathered} \tag{2.25}$$

It is worth mentioning that in the above expressions $Br << 1$. This consideration is wellmet in physical systems for example, ordinary water has the dynamic viscosity $\mu = 0.89cP$ (centi poise) and thermal conductivity $0.613W/mK$ (watt per meter Kelvin) at 25^0c ($298Kelvin \approx$ room temperature). If the characteristic speed of fluid is taken to be $1m/s$ (meter per second) and wall temperature to be $310Kelvin$ ($\approx$ equal to body temperature). The Brinkman number comes out to be $1.2787 \times 10^{-4} << 1$. In light of the expansions given through Eq. (2.25), the zeroth and first order systems take the following form:

Zeroth order system

$$B\frac{\partial^2\theta_0}{\partial y^2}+\varepsilon=0,$$
$$\frac{\partial\theta_0}{\partial y}=0,\ \text{at } y=0 \text{ and } \theta_0+\gamma\frac{\partial\theta_0}{\partial y}=0,\ \text{at } y=h, \tag{2.26}$$

$$\frac{\partial p_0}{\partial x}=\frac{1}{(1-\phi)^{2.5}}\frac{\partial^3\psi_0}{\partial y^3}+Grsin\alpha\{1-\phi+\phi(\tfrac{(\rho\beta)_p}{(\rho\beta)_f})\}\theta_0,$$
$$\psi_0=0,\frac{\partial^2\psi_0}{\partial y^2}=0,\ \text{at } y=0 \text{ and } \psi_0=f_0,\frac{\partial\psi_0}{\partial y}+\frac{\beta}{(1-\phi)^{2.5}}\frac{\partial^2\psi_0}{\partial y^2}=-1,\ \text{at } y=h. \tag{2.27}$$

First order system

$$B\frac{\partial^2\theta_1}{\partial y^2}+\frac{1}{(1-\phi)^{2.5}}(\frac{\partial^2\psi_0}{\partial y^2})^2=0,$$
$$\frac{\partial\theta_1}{\partial y}=0,\ \text{at } y=0 \text{ and } \theta_1+\gamma\frac{\partial\theta_1}{\partial y}=0,\ \text{at } y=h, \tag{2.28}$$

$$\frac{\partial p_1}{\partial x}=\frac{1}{(1-\phi)^{2.5}}\frac{\partial^3\psi_1}{\partial y^3}+Grsin\alpha\{1-\phi+\phi(\tfrac{(\rho\beta)_p}{(\rho\beta)_f})\}\theta_1,$$
$$\psi_1=0,\frac{\partial^2\psi_1}{\partial y^2}=0,\ \text{at } y=0 \text{ and } \psi_1=f_1,\frac{\partial\psi_1}{\partial y}+\frac{\beta}{(1-\phi)^{2.5}}\frac{\partial^2\psi_1}{\partial y^2}=0,\ \text{at } y=h. \tag{2.29}$$

The graphical and physical analysis of the obtained series solutions is given in preceding section.

2.8 Results and discussion

The objective of this section is to study the effects of velocity, streamlines, pressure gradient, pressure rise per wavelength, temperature and heat transfer rate for the peristaltic flow of copper-water nanofluid through their respective plots. Figures $2.1-2.4$ study the pressure gradient for variations in sundry parameters. It is perceived that pressure gradient is maximum in the wider part of the channel and minimum in the occluded region. It is also noted that pressure gradient decreases when nanoparticles volume fraction, Grashoff number and channel inclination angle are increased. Further pressure gradient increases due to large value of velocity slip parameter.

Figures $2.5-2.8$ analyze the effects of nanoparticles volume fraction, inclination of angle, Grashoff number and velocity slip parameter on the pressure rise per wavelength. It is also

examined that there are three different pumping regions such as retrograde, peristaltic and augmented pumping region.

Effects of different parameters on the axial velocity are analyzed in the Figures $2.9 - 2.12$. Figures 2.9 and 2.12 depict that the increasing value of the nanoparticles volume fraction and velocity slip parameter decrease the velocity at the center of the channel. However reverse behavior is examined near the channel walls. Increase in the Grashoff number and channel inclination angle enhances the velocity at the central part.

Streamline illustrations are given through Figures $2.13 - 2.15$. Size of the trapped bolus decreases when copper nanoparticles volume fraction and velocity slip parameter are increased.

Figures $2.16 - 2.20$ are plotted to analyze the temperature for various values of ϕ, Gr, α, β and γ. Temperature profiles have parabolic trajectory. Temperature is maximum at the channel center and decreases near the channel walls. Inclusion of nanoparticles rapidly decrease the temperature near the channel center. These parameters effect temperature near center of the channel. However, increasing value of temperature jump parameter enhances the temperature throughout the channel.

Comparison of the heat transfer rate at the boundary for ordinary water and nanofluid is given through Figures $(2.21 - 2.24)$. It is noted through these Figs. that in the presence of nanoparticles the heat transfer rate at the boundary increase for larger values of ϕ, ϵ, Gr and Br.

Property	Basefluid(water)	Nanomaterials(copper)
Density (kg/m^3)	997.1	8933
Thermal conductivity (W/mk)	0.613	400
Specific heat (j/kgK)	4179	385
Thermal expansion coefficient (1/k)10^{-6}	210	16.65

Table 2.1: Statistical data of the thermo-physical properties [19].

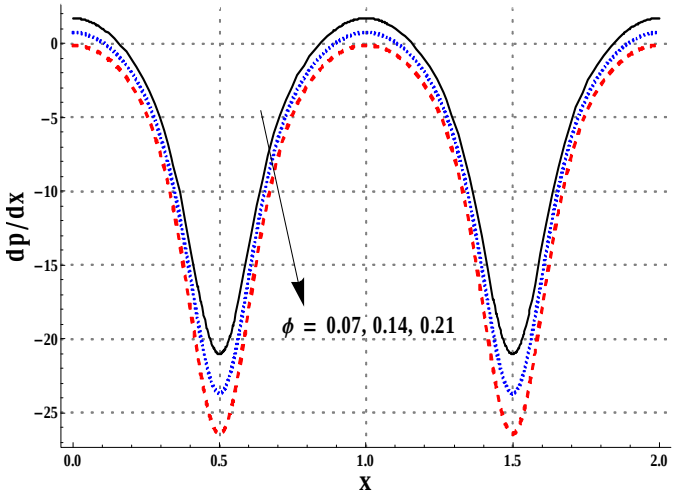

Figure 2.1. Pressure gradient for different ϕ when $\alpha = \frac{\pi}{4}$, $a = 0.6$, $\eta = 0.95$, $Br = 0.3$, $Gr = 5.0$, $\gamma = 0.1$, $\beta = 0.3$ and $\varepsilon = 1.0$.

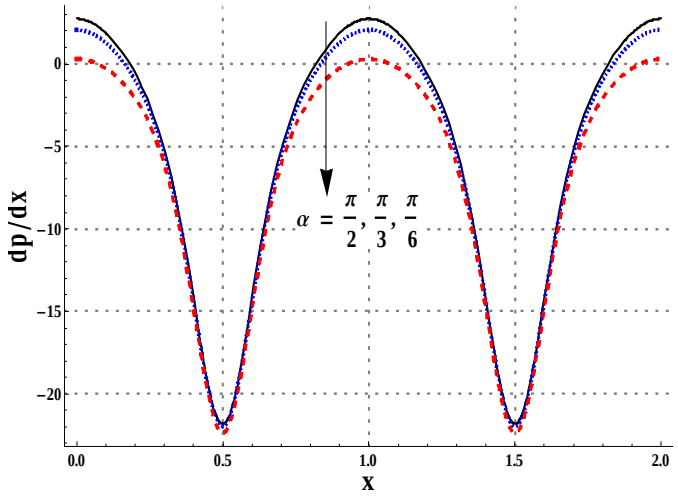

Figure 2.2. Pressure gradient for various α when $a = 0.6$, $\eta = 0.95$, $Gr = 5.0$, $\phi = 0.1$, $Br = 0.3$, $\gamma = 0.1$, $\beta = 0.3$ and $\varepsilon = 1.0$.

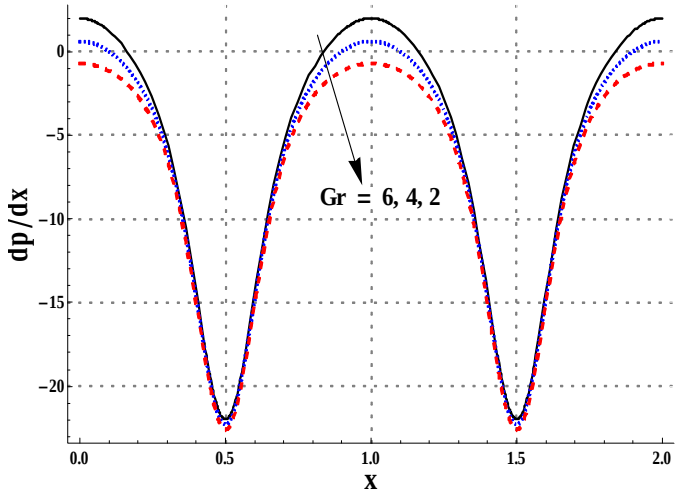

Figure 2.3. Pressure gradient for change in Gr when $\alpha = \frac{\pi}{4}$, $a = 0.6$, $\eta = 0.95$, $\phi = 0.1$, $Br = 0.3$, $\gamma = 0.1$, $\beta = 0.3$ and $\varepsilon = 1.0$.

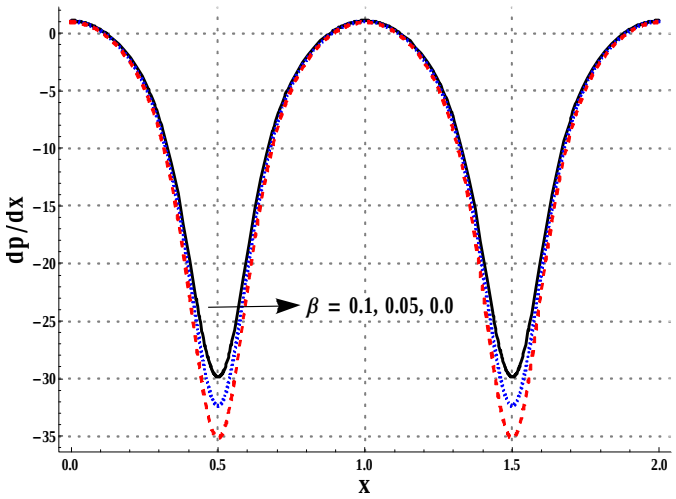

Figure 2.4. Pressure gradient for different values of β when $\alpha = \frac{\pi}{4}$, $a = 0.6$, $\eta = 0.95$, $Gr = 5.0$, $\phi = 0.1$, $Br = 0.3$, $\gamma = 0.1$ and $\varepsilon = 1.0$.

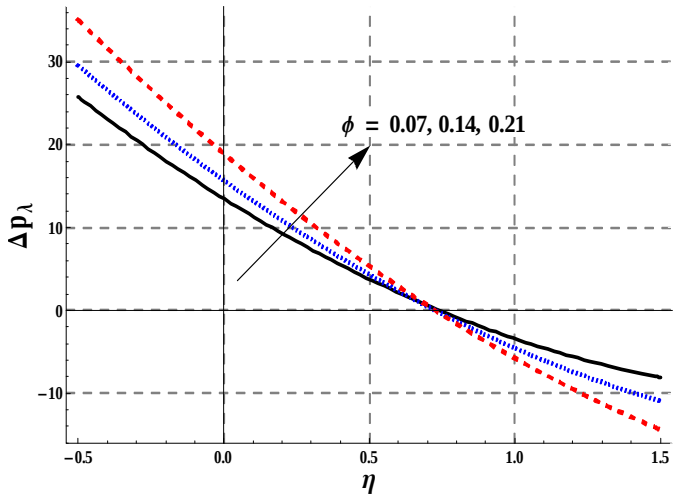

Figure 2.5. ΔP_λ for various values of ϕ when $\alpha = \frac{\pi}{4}$, $a = 0.1$, $Gr = 5.0$, $Br = 0.3$, $\gamma = 0.1$, $\beta = 0.3$ and $\varepsilon = 1.0$.

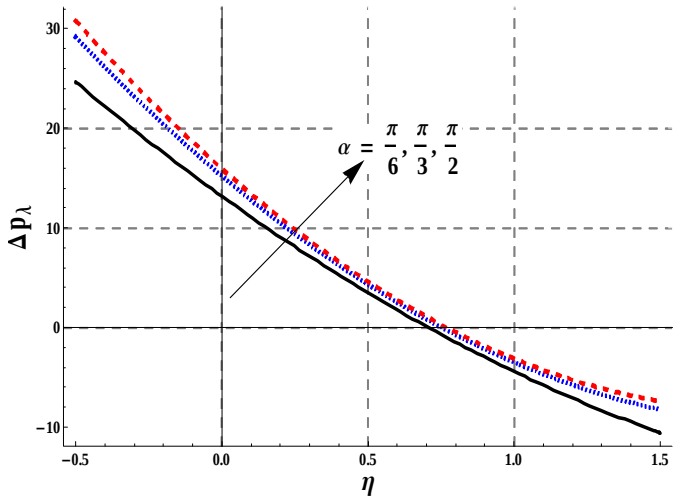

Figure 2.6. ΔP_λ for various values of α when $a = 0.1$, $Gr = 5.0$, $\phi = 0.1$, $Br = 0.3$, $\gamma = 0.1$, $\beta = 0.3$ and $\varepsilon = 1.0$.

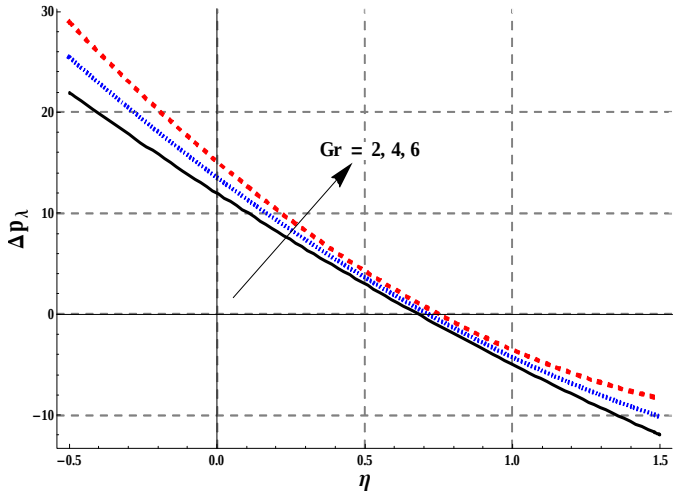

Figure 2.7. ΔP_λ for various values of Gr when $\alpha = \frac{\pi}{4}$, $a = 0.1$, $\phi = 0.1$, $Br = 0.3$, $\gamma = 0.1$, $\beta = 0.3$ and $\varepsilon = 1.0$.

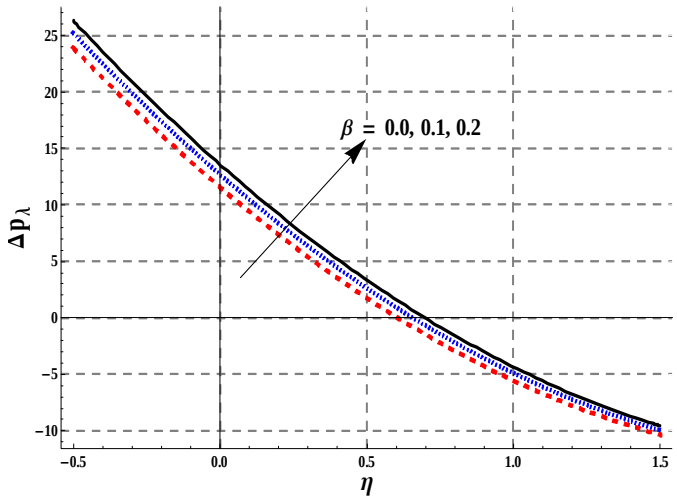

Figure 2.8. ΔP_λ for various values of β when $\alpha = \frac{\pi}{4}$, $a = 0.1$, $Gr = 5.0$, $\phi = 0.1$, $Br = 0.3$, $\gamma = 0.1$ and $\varepsilon = 1.0$.

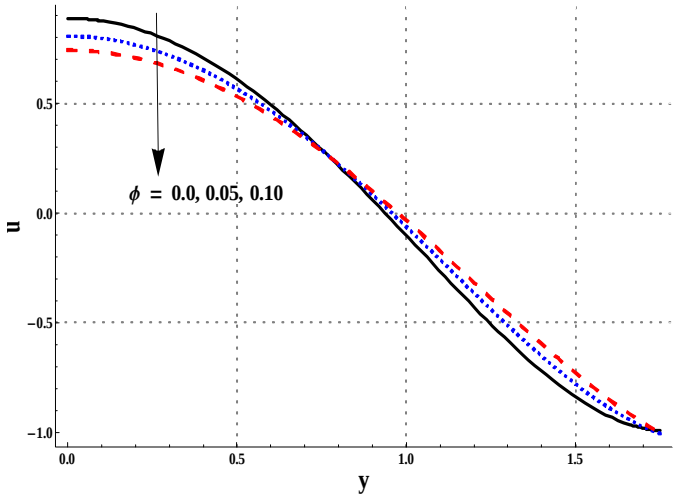

Figure 2.9. Effect of ϕ on axial velocity when $\alpha = \frac{\pi}{4}$, $a = 0.6$, $\eta = 1.2$, $Gr = 5.0$, $x = 1.0$, $Br = 0.3$, $\gamma = 0.1$, $\beta = 0.1$ and $\varepsilon = 1.0$.

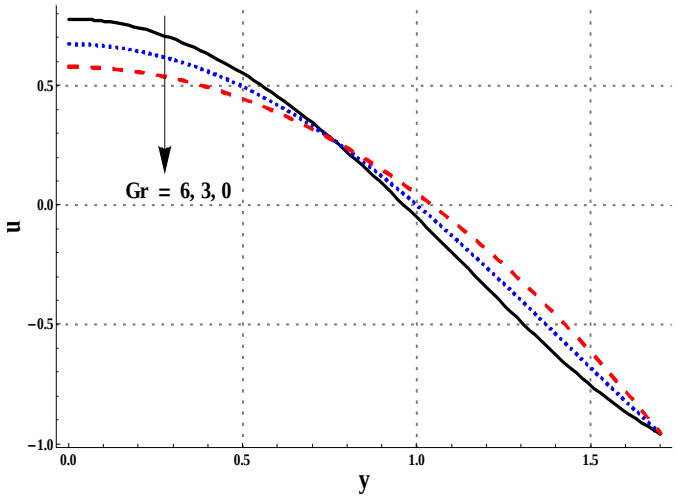

Figure 2.10. Effects of Gr on axial velocity when $\alpha = \frac{\pi}{4}$, $a = 0.6$, $\eta = 1.2$, $x = 0$, $\phi = 0.1$, $Br = 0.3$, $\gamma = 0.1$, $\beta = 0.3$ and $\varepsilon = 1.0$.

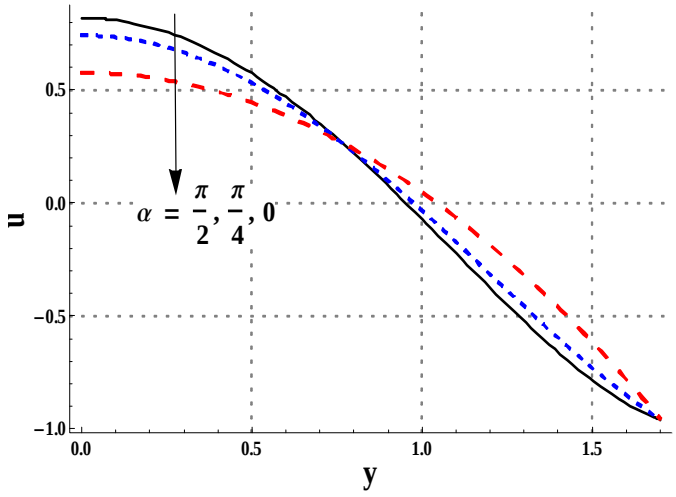

Figure 2.11. Effects of α on axial velocity when $a = 0.6$, $\eta = 1.2$, $x = 1.0$, $Gr = 5.0$, $\phi = 0.1$, $Br = 0.3$, $\gamma = 0.1$, $\beta = 0.1$ and $\varepsilon = 1.0$.

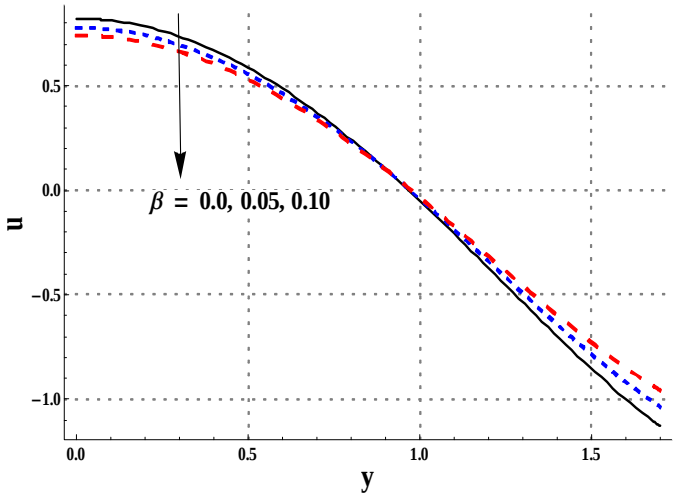

Figure 2.12. Effects of β on axial velocity when $\alpha = \frac{\pi}{4}$, $a = 0.6$, $\eta = 1.2$, $x = 1.0$, $Gr = 5.0$, $\phi = 0.1$, $Br = 0.3$, $\gamma = 0.1$ and $\varepsilon = 1.0$.

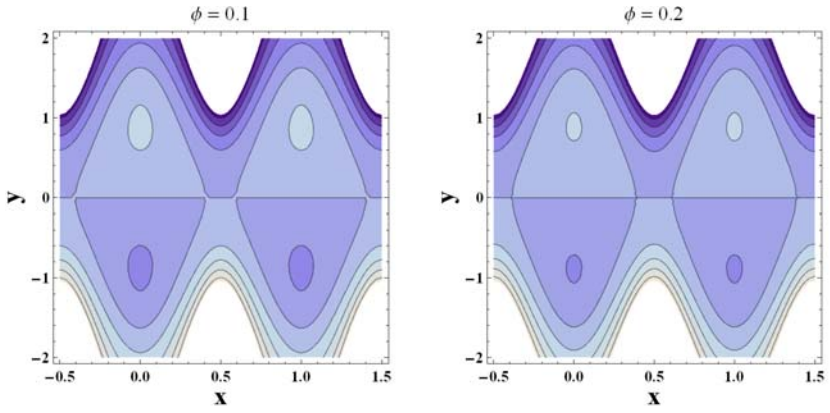

Figure 2.13. Illustrations of streamlines when $\alpha = \frac{\pi}{4}$, $a = 0.7$, $\eta = 0.95$, $Gr = 5.0$, $Br = 0.3$, $\gamma = 0.1$, $\beta = 0.3$ and $\varepsilon = 1.0$.

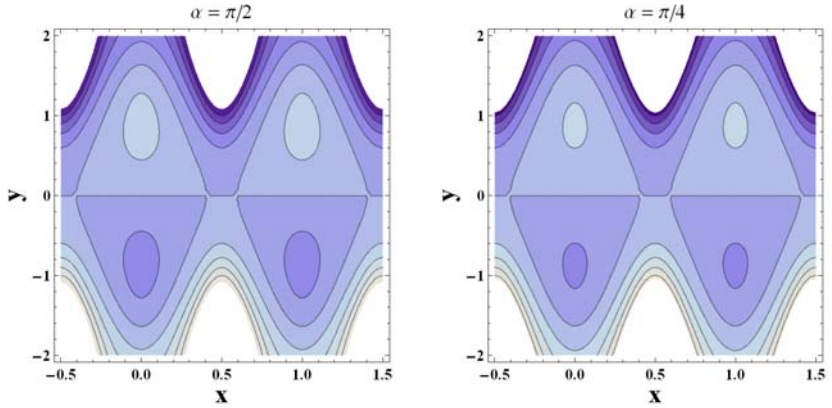

Figure 2.14. Illustrations of streamlines when $\alpha = \frac{\pi}{4}$, $a = 0.7$, $\eta = 0.95$, $\phi = 0.1$, $Gr = 5.0$, $Br = 0.3$, $\gamma = 0.1$, $\beta = 0.3$ and $\varepsilon = 1.0$.

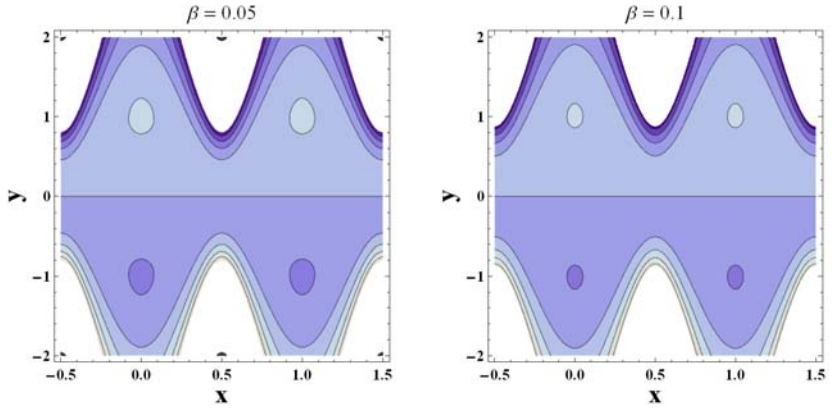

Figure 2.15. Illustration of streamlines when $\alpha = \frac{\pi}{4}$, $a = 0.7$, $\eta = 1.2$, $\phi = 0.1$, $Gr = 5.0$, $Br = 0.3$, $\gamma = 0.1$ and $\varepsilon = 1.0$.

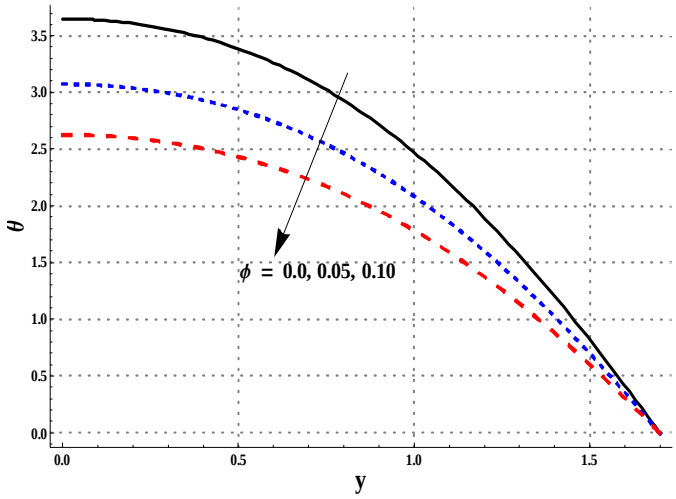

Figure 2.16. Effects of ϕ on θ when $\alpha = \frac{\pi}{4}$, $a = 0.6$, $\eta = 1.2$, $x = 1.0$, $Gr = 5.0$, $Br = 0.3$, $\gamma = 0.1$, $\beta = 0.1$ and $\varepsilon = 2.0$.

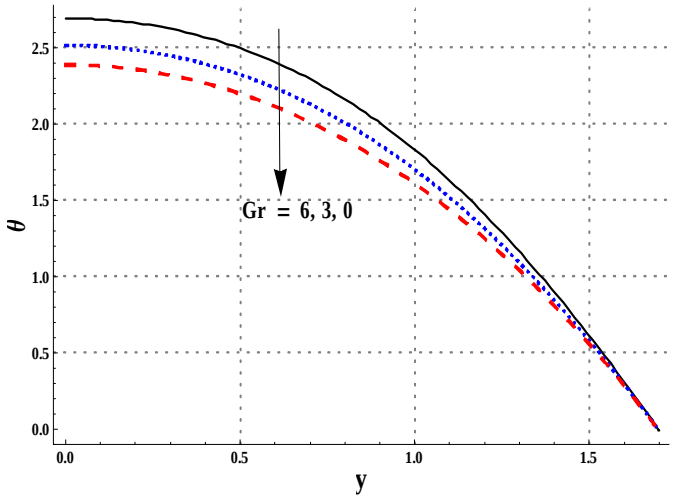

Figure 2.17. Effects of Gr on θ when $\alpha = \frac{\pi}{4}$, $a = 0.6$, $\eta = 1.2$, $x = 1.0$, $\phi = 0.1$, $Br = 0.3$, $\gamma = 0.1$, $\beta = 0.1$ and $\varepsilon = 2.0$.

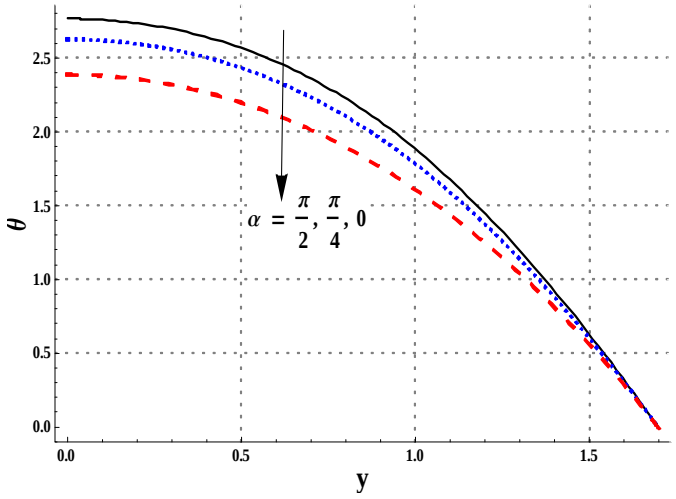

Figure 2.18. Effects of α on θ when $a = 0.6$, $\eta = 1.2$, $x = 1.0$, $\phi = 0.1$, $Gr = 5.0$, $Br = 0.3$, $\gamma = 0.1$, $\beta = 0.1$ and $\varepsilon = 2.0$.

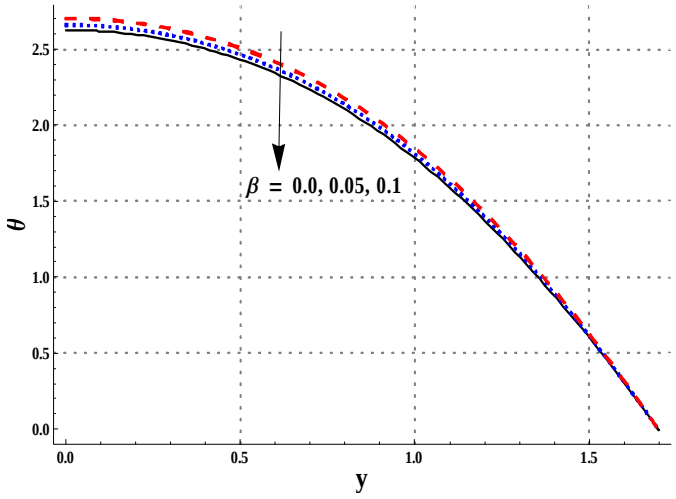

Figure 2.19. Effects of β on θ when $\alpha = \frac{\pi}{4}$, $a = 0.6$, $\eta = 1.2$, $x = 1.0$, $Gr = 5.0$, $\phi = 0.1$, $Br = 0.3$, $\gamma = 0.1$ and $\varepsilon = 2.0$.

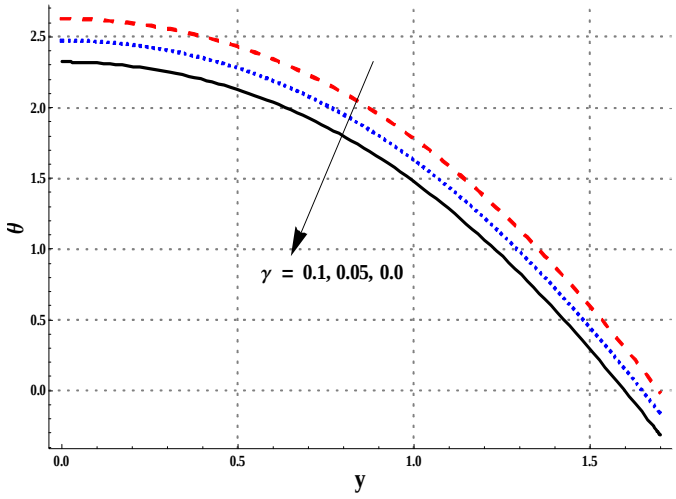

Figure 2.20. Effects of γ on θ when $\alpha = \frac{\pi}{4}$, $a = 0.6$, $\eta = 1.2$, $x = 1.0$, $Gr = 5.0$, $\phi = 0.1$, $Br = 0.3$ $\beta = 0.1$ and $\varepsilon = 2.0$.

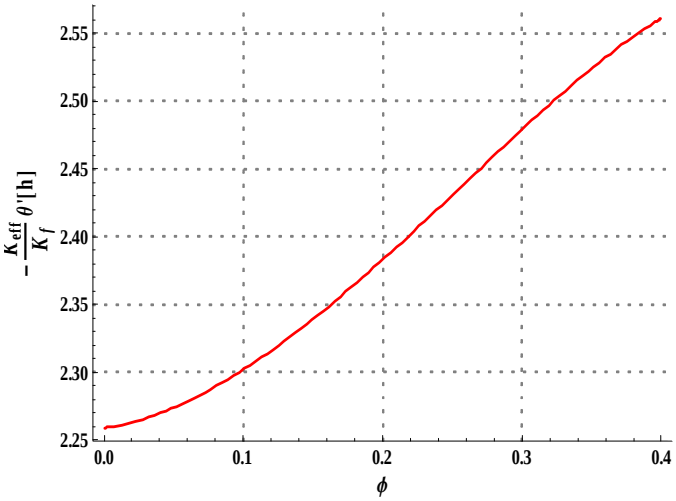

Figure 2.21. Effects of ϕ on heat transfer rate when $\alpha = \frac{\pi}{4}$, $a = 0.6$, $\eta = 1.2$, $x = 1.0$, $Gr = 5.0$, $Br = 0.3$, $\gamma = 0.1$, $\beta = 0.1$ and $\varepsilon = 1.0$.

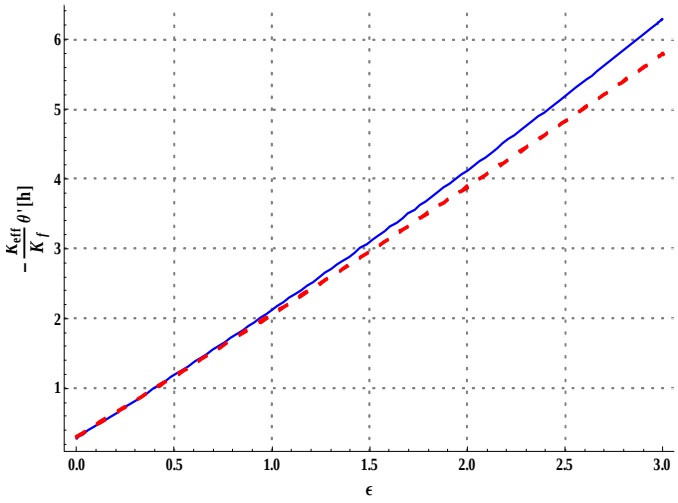

Figure 2.22. Effects of ε on heat transfer rate when $\alpha = \frac{\pi}{4}$, $a = 0.6$, $\eta = 1.2$, $x = 1.0$, $Gr = 5.0$, $Br = 0.3$, $\gamma = 0.1$, and $\beta = 0.3$.

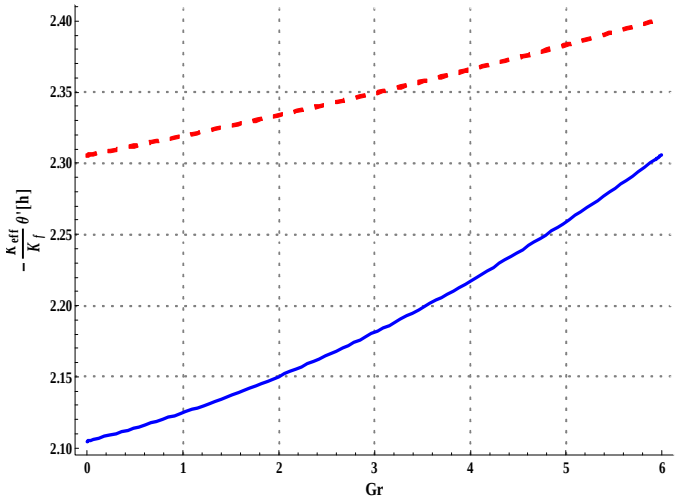

Figure 2.23. Effects of Gr on heat transfer rate when $\alpha = \frac{\pi}{4}$, $a = 0.6$, $\eta = 1.2$, $x = 1.0$, $Br = 0.3$, $\gamma = 0.1$, $\beta = 0.1$ and $\varepsilon = 1.0$.

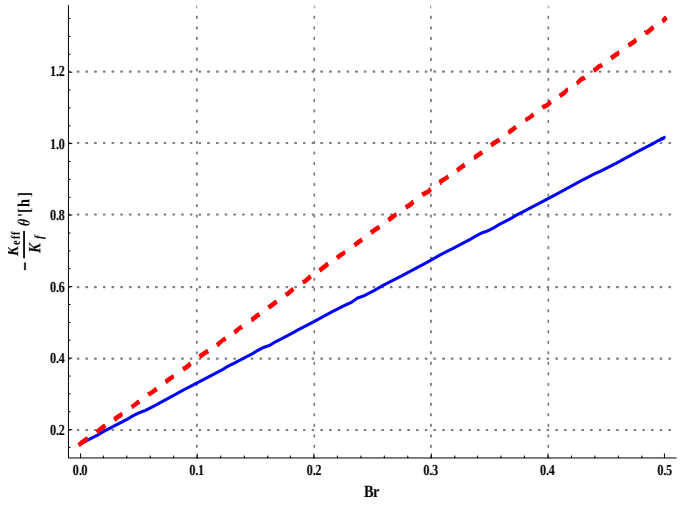

Figure 2.24. Effects of Br on heat transfer rate when $\alpha = \frac{\pi}{4}$, $a = 0.6$, $\eta = 1.2$, $x = 1.0$, $Gr = 5.0$, $\gamma = 0.1$, $\beta = 0.1$ and $\varepsilon = 0.1$.

Chapter 3

Peristalsis of single walled carbon nanotubes with different thermal conductivity models

3.1 Introduction

Analysis here studies the influences for single walled carbon nanotubes (SWCNTs) on the peristaltic motion. Mixed convective flow in symmetric channel is taken. Heat source/sink is also present. Further velocity slip and temperature jump conditions. Maxewell's [22], the Hamilton-Crosser's [23] and the Xue's [24] models for the thermal conductivity of the nanomaterials are used here.

3.2 Physical model

Consider an incompressible nanofluid (composed of water and the SWCNTs) in a symmetric channel of width $2d$. Coordinate system is selected in such a manner that the $\overline{X}-$axis lies along the length of channel and the $\overline{Y}-$ axis normal to the $\overline{X}-$ axis. The channel is inclined at an angle "α" with the horizontal. Flow is created by sinusoidal travelling waves of wavelength λ and constant speed c. Fig. 3.1 consists of physical model. The mathematical form of the peristaltic walls is given by

$$\pm\overline{H}(\bar{X},\bar{t}) = \pm d \pm a_1 cos(\frac{2\pi}{\lambda}(\bar{X} - c\bar{t})). \tag{3.1}$$

Here a_1 denotes the amplitude, $\bar{t}$ the time, $+ve$ and $-ve$ signs indicate the values for the walls in the positive and negative $\overline{Y}$-directions respectively.

Effective viscosity μ_{eff}, density of nanofluid ρ_{nf}, effective thermal expansion coefficient β_{nf} and effective heat capacity $(\rho C)_{nf}$ of the nanofluid [19] are given as follows:

$$\begin{gathered}\mu_{eff} = \frac{\mu_f}{(1-\phi)^{2.5}}, \rho_{nf} = (1-\phi)\rho_f + \phi\rho_p, \\ (\rho C)_{nf} = (1-\phi)(C\rho)_f + \phi(C\rho)_p, (\rho\beta)_{nf} = (1-\phi)\rho_f\beta_f + \phi\rho_p\beta_p.\end{gathered} \tag{3.2}$$

In these equations ρ denotes the density, β the thermal expansion coefficient, μ the viscosity and C the specific heat. The subscripts "p" and "f" denote the nanotubes and water phase respectively. The effective thermal conductivity (K_{eff}) is given as follows:

$$\begin{gathered}\frac{K_{eff}}{K_f} = \frac{K_p + 2K_f - 2\phi(K_f - K_p)}{K_p + 2K_f + \phi(K_f - K_p)} \text{for Maxewell's model (Eq.1.8),} \\ \frac{K_{eff}}{K_f} = \frac{K_p + (n-1)K_f - (n-1)\phi(K_f - K_p)}{K_p + (n-1)K_f + \phi(K_f - K_p)} \text{ for H-C's model (Eq. 1.9) and} \\ \frac{K_{eff}}{K_f} = \frac{1 - \phi + 2\phi\frac{K_{CNT}}{K_{CNT}\text{-}K_f}[\ln\frac{K_{CNT}+K_f}{2K_f}]}{1 - \phi + 2\phi\frac{K_f}{K_{CNT}\text{-}K_f}[\ln\frac{K_{CNT}+K_f}{2K_f}]} \text{ for Xue's model (Eq. 1.10).}\end{gathered} \tag{3.3}$$

Numerical values of the thermophysical properties of water and nanomaterials can be seen through Table **3.1**.

3.3 Governing equations in the wave frame

Note that channel boundaries have temperature T_0. For two dimensional flow, $\overline{U}(\overline{X},\overline{Y},\overline{t})$ and $\overline{V}(\overline{X},\overline{Y},\overline{t})$ are the $\overline{X}$ and $\overline{Y}$ components of velocity and $\overline{P}(\overline{X},\overline{Y},\overline{t})$ the pressure in the laboratory frame. The variables and quantities in laboratory $(\overline{X},\overline{Y},\overline{t})$ and wave frames $(\overline{x},\overline{y})$ for the present flow phenomena are

$$\bar{x} = \bar{X} - c\bar{t}, \bar{y} = \bar{Y}, \bar{u} = \bar{U} - c, \bar{v} = \bar{V}, \bar{p}(\bar{x},\bar{y}) = \bar{P}(\bar{X},\bar{Y},\bar{t}), \tag{3.4}$$

where $\bar{u}$ and $\bar{v}$ depict the longitudinal and transverse components of the velocity and $\bar{p}(\bar{x},\bar{y})$ is the pressure in the wave frame. The relevant equations here are given by

$$\frac{\partial \bar{u}}{\partial \bar{x}}+\frac{\partial \bar{v}}{\partial \bar{y}}=0, \tag{3.5}$$

$$\begin{aligned}((1-\phi)\rho_f+\phi\rho_p)((\bar{u}+c)\frac{\partial}{\partial \bar{x}}+\bar{v}\frac{\partial}{\partial \bar{y}})(\bar{u}+c)=-\frac{\partial \bar{p}}{\partial \bar{x}}+\frac{\mu_f}{(1-\phi)^{2.5}}(\frac{\partial^2 \bar{u}}{\partial \bar{x}^2}+\frac{\partial^2 \bar{u}}{\partial \bar{y}^2})\\ +g((1-\phi)\rho_f\beta_f+\phi\rho_p\beta_p)(T-T_0)sin\alpha,\end{aligned} \tag{3.6}$$

$$\begin{aligned}((1-\phi)\rho_f+\phi\rho_p)((\bar{u}+c)\frac{\partial}{\partial \bar{x}}+\bar{v}\frac{\partial}{\partial \bar{y}})\bar{v}=-\frac{\partial \bar{p}}{\partial \bar{y}}+\frac{\mu_f}{(1-\phi)^{2.5}}(\frac{\partial^2 \bar{v}}{\partial \bar{x}^2}+\frac{\partial^2 \bar{v}}{\partial \bar{y}^2})\\ +g((1-\phi)\rho_f\beta_f+\phi\rho_p\beta_p)(T-T_0)cos\alpha,\end{aligned} \tag{3.7}$$

$$\begin{aligned}((1-\phi)(C\rho)_f+\phi(C\rho)_p)((\bar{u}+c)\frac{\partial}{\partial \bar{x}}+\bar{v}\frac{\partial}{\partial \bar{y}})T=K_{eff}(\frac{\partial^2 T}{\partial \bar{x}^2}+\frac{\partial^2 T}{\partial \bar{y}^2})\\ +\Phi+\frac{\mu_f}{(1-\phi)^{2.5}}[2((\frac{\partial \bar{u}}{\partial \bar{x}})^2+(\frac{\partial \bar{v}}{\partial \bar{y}})^2)+(\frac{\partial \bar{u}}{\partial \bar{y}}+\frac{\partial \bar{v}}{\partial \bar{x}})^2].\end{aligned} \tag{3.8}$$

Here g represents the acceleration due to gravity and T the nanofluid temperature.

3.4 Non-dimensionalization of the problem

Making use of the following dimensionless quantities

$$\begin{aligned}x=\frac{\overline{x}}{\lambda},y=\frac{\overline{y}}{d},u=\frac{\overline{u}}{c},v=\frac{\overline{v}}{c\delta},\delta=\frac{d}{\lambda},h=\frac{\overline{H}}{d},a=\frac{a_1}{d},p=\frac{d^2\overline{p}}{c\lambda\mu_f},\\ \upsilon=\frac{\mu_f}{\rho_f},Re=\frac{\rho_f\ cd}{\mu_f},t=\frac{ct}{\lambda},E=\frac{c^2}{C_fT_0},pr=\frac{\mu_fC_f}{K_f},Gr=\frac{\rho_fg\beta_fT_0d^2}{\mu_fc},\\ \theta=\frac{T-T_0}{T_0},Br=PrE,\varepsilon=\frac{d^2\Phi}{T_0K_f},u=\frac{\partial \psi}{\partial y},v=-\frac{\partial \psi}{\partial x},\end{aligned} \tag{3.9}$$

and adopting large wavelength and small Reynolds number analysis we have

$$\frac{\partial p}{\partial x}=\frac{1}{(1-\phi)^{2.5}}\frac{\partial^3 \psi}{\partial y^3}+Grsin\alpha\{1-\phi+\phi(\frac{(\rho\beta)_p}{(\rho\beta)_f})\}\theta, \tag{3.10}$$

$$p_y=0, \tag{3.11}$$

$$B\frac{\partial^2 \theta}{\partial y^2}+\frac{Br}{(1-\phi)^{2.5}}(\frac{\partial^2 \psi}{\partial y^2})^2+\varepsilon=0. \tag{3.12}$$

Here δ, α, p, υ, Re, E, Pr, Gr, θ, Br, ϵ and ψ denote the wave number, inclination angle, pressure, kinematic viscosity, Reynolds number, Eckert number, Prandtl number, Grashoff number, dimensionless temperature, Brinkman number, dimensionless heat generation/ absorption parameter and stream function respectively. Further Eq. (3.11) indicates that pressure is not a function of "y" and the continuity equation (Eq. 3.5) is identically satisfied. Here "B" is defined as follows:

$$B = \frac{K_{eff}}{K_f} \tag{3.13}$$

Cross differentiation of (3.10) and (3.11) yields

$$0 = \frac{1}{(1-\phi)^{2.5}} \frac{\partial^4 \psi}{\partial y^4} + Gr sin\alpha \{1 - \phi + \phi(\frac{(\rho\beta)_p}{(\rho\beta)_f})\} \frac{\partial \theta}{\partial y}. \tag{3.14}$$

3.5 Volume flow rate and boundary conditions

Velocity slip condition

In the fixed frame of reference the slip conditions at the wall are defined as

$$\bar{U}(\bar{X}, \bar{H}, \bar{t}) - \bar{U}_w = \tilde{n}\beta_1 \bar{\tau}_{XY}, \tag{3.15}$$

in which $\bar{U}(\bar{X}, \bar{Y}, \bar{t})$ is the longitudinal velocity in laboratory frame, $\bar{\tau}_{XY}$ the shear stress, β_1 the dimensional velocity slip parameter, $\tilde{n}$ the unit normal on the wall and U_w velocity of the walls. Transforming the above expressions in the wave frame through Eq. (3.4) we obtain

$$u(\bar{x}, \bar{h}) - c = \tilde{n}\beta_1 \bar{\tau}_{xy}. \tag{3.16}$$

Here dimensionless boundary conditions in the wave frame are given as:

$$\begin{gathered} \psi = 0, \frac{\partial^2 \psi}{\partial y^2} = 0 \text{ at } y = 0, \\ \psi = F, \frac{\partial \psi}{\partial y} + \frac{\beta}{(1-\phi)^{2.5}} \frac{\partial^2 \psi}{\partial y^2} = -1 \text{ at } y = h, \end{gathered} \tag{3.17}$$

in which $\beta (= \frac{\beta_1 \mu}{d})$ is the dimensionless velocity slip parameter.

Temperature jump condition

In the laboratory frame of reference the temperature jump condition at the walls is defined

as

$$\bar{T} - \bar{T}_w = \tilde{n}\gamma_1 \frac{\partial \bar{T}}{\partial \bar{y}} \tag{3.18}$$

$\bar{T}$ is the temperature of fluid, γ the thermal slip parameter, $\tilde{n}$ the unit normal on the walls and $\bar{T}_w (= T_0)$ is the temperature of the walls. The non-dimensional form for temperature are given by

$$\begin{aligned} \tfrac{\partial \theta}{\partial y} = 0 \text{ at } y = 0, \\ \theta + \gamma \tfrac{\partial \theta}{\partial y} = 0 \text{ at } y = h. \end{aligned} \tag{3.19}$$

Here $\gamma (= \frac{\gamma_1}{d})$ is the dimensionless temperature jump parameter.

Flow rate

For laboratory frame the flow rate is

$$Q = \int_0^{\bar{H}(\bar{x},t)} \bar{U}(\bar{X}, \bar{Y}, \bar{t}) d\bar{Y}, \tag{3.20}$$

where $\bar{H}$ is a function of $\bar{X}$ and $\bar{t}$. In wave frame the above expression is reduced to

$$q = \int_0^{\bar{h}(\bar{x})} \bar{u}(\bar{x}, \bar{y}) d\bar{y}, \tag{3.21}$$

where $\bar{h}$ is a function of x. Using Eqs.(3.9) and (3.21) we have

$$Q = q + c\bar{h}(x) \tag{3.22}$$

The time mean flow can be written as

$$\bar{Q} = \frac{1}{T} \int_0^T Q dt, \tag{3.23}$$

in which T is the period. Putting Eq. (3.22) into the above expression and integrating we obtain

$$\bar{Q} = q + cd. \tag{3.24}$$

We define F and η as the dimensionless mean flows in the wave and laboratory frames by

$$\eta = \frac{\bar{Q}}{cd}, F = \frac{\bar{q}}{cd}, \tag{3.25}$$

the two flow rates are related through the following relation:

$$\eta = F + 1 \tag{3.26}$$

where

$$F = \int_0^h \frac{\partial \psi}{\partial y} dy. \tag{3.27}$$

Boundary conditions in non-dimensional form

The boundary conditions for the existing flow configuration here are given as:

$$\begin{gathered} \psi = 0, \psi_{yy} = 0, \theta_y = 0, \text{ at } y = 0, \\ \psi = F, \frac{\partial \psi}{\partial y} + \frac{\beta}{(1-\phi)^{2.5}} \frac{\partial^2 \psi}{\partial y^2} = -1, \theta + \gamma \frac{\partial \theta}{\partial y} = 0, \text{ at } y = h, \end{gathered} \tag{3.28}$$

where $h = 1 + a\ cos(2\pi x)$ is the dimensionless wall shape, β is the dimensionless velocity slip parameter and γ the dimensionless temperature jump parameter. Pressure rise per wavelength (ΔP_λ) is

$$\Delta P_\lambda = \int_0^1 (\frac{dp}{dx}) dx. \tag{3.29}$$

3.6 Series solutions

We expand the flow quantities via "Br" as follows:

$$\psi = \psi_0 + Br\psi_1 + O(Br^2) + ...,$$

$$\theta = \theta_0 + Br\theta_1 + O(Br^2) + ...,$$

$$p = p_0 + Brp_1 + O(Br^2) + ...,$$

$$F = f_0 + Brf_1 + O(Br^2) + ...$$

Making use of the above mentioned expansions, the zeroth and the first order systems take the following forms:

Zeroth order system

$$\begin{gathered} B\frac{\partial^2\theta_0}{\partial y^2}+\varepsilon=0, \\ \frac{\partial\theta_0}{\partial y}=0,\ \text{at } y=0 \text{ and } \theta_0+\gamma\frac{\partial\theta_0}{\partial y}=0,\ \text{at } y=h, \end{gathered} \tag{3.30}$$

$$\begin{gathered} \frac{\partial p_0}{\partial x}=\frac{1}{(1-\phi)^{2.5}}\frac{\partial^3\psi_0}{\partial y^3}+Grsin\alpha\{1-\phi+\phi(\tfrac{(\rho\beta)_p}{(\rho\beta)_f})\}\theta_0, \\ \psi_0=0, \frac{\partial^2\psi_0}{\partial y^2}=0,\ \text{at } y=0 \text{ and } \psi_0=f_0, \frac{\partial\psi_0}{\partial y}+\frac{\beta}{(1-\phi)^{2.5}}\frac{\partial^2\psi_0}{\partial y^2}=-1,\ \text{at } y=h. \end{gathered} \tag{3.31}$$

First order system

$$\begin{gathered} B\frac{\partial^2\theta_1}{\partial y^2}+\frac{1}{(1-\phi)^{2.5}}(\frac{\partial^2\psi_0}{\partial y^2})^2=0, \\ \frac{\partial\theta_1}{\partial y}=0,\ \text{at } y=0 \text{ and } \theta_1+\gamma\frac{\partial\theta_1}{\partial y}=0,\ \text{at } y=h, \end{gathered} \tag{3.32}$$

$$\begin{gathered} \frac{\partial p_1}{\partial x}=\frac{1}{(1-\phi)^{2.5}}\frac{\partial^3\psi_1}{\partial y^3}+Grsin\alpha\{1-\phi+\phi(\tfrac{(\rho\beta)_p}{(\rho\beta)_f})\}\theta_1, \\ \psi_1=0, \frac{\partial^2\psi_1}{\partial y^2}=0,\ \text{at } y=0 \text{ and } \psi_1=f_1, \frac{\partial\psi_1}{\partial y}+\frac{\beta}{(1-\phi)^{2.5}}\frac{\partial^2\psi_1}{\partial y^2}=0,\ \text{at } y=h. \end{gathered} \tag{3.33}$$

Detailed analysis of the obtained series solutions is provided in the next section.

3.7 Discussion and comparison of the results

For the sake of simplicity the discussion of the results has been divided into subsections. Each subsection consists of the analysis of one particular physical quantity.

3.7.1 Pressure gradient

Pressure gradient for variations in the values of different flow parameters is analyzed through Figs. $3.2-3.5$. These Figs. present that the pressure gradient has an oscillatory behavior with maximum value near the wider part of the channel. Fig. 3.2 indicates that the pressure gradient is decreasing function of SWCNTs volume fraction in all parts of channel. Larger channel inclination angle correspond to much pressure gradient in the wider part of channel

(see Fig. 3.3). Similarly for an increase in the Grashoff number, the pressure gradient increases in the wider part of channel (see Fig. 3.4). However in the narrow part of the channel not much influence of α and Gr on the pressure gradient is noted. Fig. 3.5 present the behavior of pressure gradient for various values of velocity slip parameter. Enhancement in velocity slip parameter results in the increase of pressure gradient in the wider part of channel only.

3.7.2 Pressure rise per wavelength

Figs. $3.6 - 3.9$ show the features of pressure rise per wavelength versus flow rate for CNT's volume fraction, inclination angle, Grashoff number and velocity slip parameter. Through these Figs. it is analyzed that when flow rate increases, then pressure rise per wavelength decreases. Fig. 3.6 shows that higher values of the CNTs volume fraction result in enhancement of pressure rise per wavelength in the retrograde pumping region. However the opposite behavior is observed in the augmented pumping region for pressure rise per wavelength. Fig. 3.7 depicts the variation of pressure rise per wavelength for various values of the inclination angle. It is seen through this Fig. that higher values of the angle of inclination result in enhancement of pressure rise per wavelength in the retrograde pumping region and opposite behavior is observed in the augmented pumping region. Pressure rise per wavelength for variations in the Grashoff number is examined through Fig. 3.8. This Fig. indicates that an increase in the Grashoff number enhances the pressure rise per wavelength. Pressure rise per wavelength decreases with an increase in the velocity slip parameter (see Fig. 3.9).

3.7.3 Axial velocity and streamlines

Figs. $3.10 - 3.13$ show behavior of axial velocity corresponding to change in the CNTs volume fraction, Grashoff number, channel inclination angle and velocity slip parameter. It is noted through these Figs. that the velocity has maximum value near the center of the channel. Fig. 3.10 shows the axial velocity for different values of the CNTs volume fraction. Higher values of CNT's results in the reduction of velocity field. In fact, higher values of CNTs provide more resistance to the fluid motion, but near the wall the velocity decreases due to slip effects. Fig. 3.11 shows the characteristics of velocity field for different values of Grashoff number. Velocity is increasing function of Grashoff number at the center but it decreases near the channel walls

for larger Grashoff number. When channel inclination is increased the velocity enhances near the center of the channel, but reverse situation is observed near the wall (see Fig. 3.12). From Fig. 3.13 it is noted that with an increase in the velocity slip parameter the velocity field enhances near the channel wall and reverse situation is noted at the center of channel. It is seen from Fig. 3.14 that increase in the CNTs volume fraction decreases the size of the trapped bolus. The size of trapped bolus slightly reduces for larger inclination of channel (see Fig. 3.15). When velocity slip parameter increases then the size of bolus enhances (see Fig. 3.16).

3.7.4 Heat transfer analysis

Figs. $3.17 - 3.21$ show the impact of various parameters on temperature profile. It is noted through these plots that temperature is maximum at the center and reverse is noted near the channel walls. Fig. 3.17 indicates that increase in CNTs volume fraction results in an increase of temperature of nanofluid. It is mainly due to the fact that for large CNTs volume fraction the effective thermal conductivity of the nanofluid increases and it plays effective role in cooling the nanofluid within the channel. Higher values of Grashoff number results in enhancement of temperature (see Fig. 3.18). It is observed from Fig. 3.19 that temperature is an increasing function of channel inclination. However the heat transfer rate decreases. Increase in velocity slip parameter reduces temperature of nanofluid (see Fig. 3.20). Fig. 3.21 shows that larger thermal slip parameter leads to an increase in temperature of nanofluid. Fig. 2.22 represent the heat transfer rate for variation of CNTs volume fraction at the wall. It is noted that when CNTs volume fraction is increasing then heat transfer rate enhances. In fact CNT's is used as an agent of rapid heat transfer.

3.7.5 Comparison

One of the prime goals of this analysis is to provide a comparison between the peristaltic flow of the copper nanoparticles and the SWCNTs through Tables **3.2-3.4**. Table **3.2** gives the numerical values of the maximum velocity near the center of the channel. Such values are obtained for both the copper nanoparticles and the SWCNTs. It is observed through this table that the velocity near the center of channel for the copper nanoparticles is more when compared to SWCNTs. Further the Maxwell's model predicts larger values of the velocity near

the center of channel. Table **3.3** indicates the numerical values of temperature near the center of channel. It is observed through this table that the nanofluid composed of the SWCNTs have lower temperature in comparison to nanofluid composed of the copper nanoparticles. Also this difference in maximum temperature decreases with an increase in the value of volume fraction of SWCNTs/Cu nanoparticles. Numerical values of heat transfer rate at the wall for the copper nanoparticles and the SWCNTs are given through table **3.4**. This table shows that the heat transfer rate at the boundary for the SWCNTs is less when compared with that of the Cu nanoparticles.

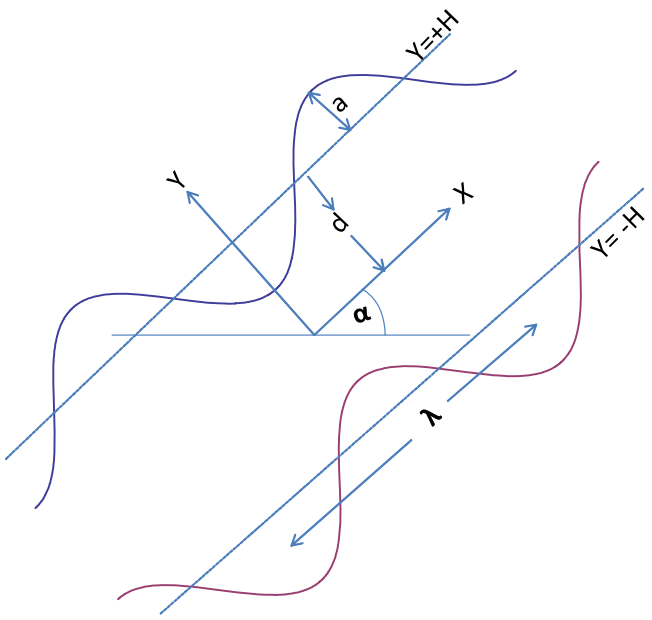

Figure 3.1. Geometry of the problem.

Property	Basefluid(water)	Nanomaterials(copper)	CNT's
Density (kg/m^3)	997.1	8933	2200
Thermal conductivity (W/mk)	0.613	400	2000
Specific heat (j/kgK)	4179	385	709
Thermal expansion coefficient (1/k)10^{-6}	210	16.65	15

Table 3.1: Statistical data of the thermo-physical properties [25].

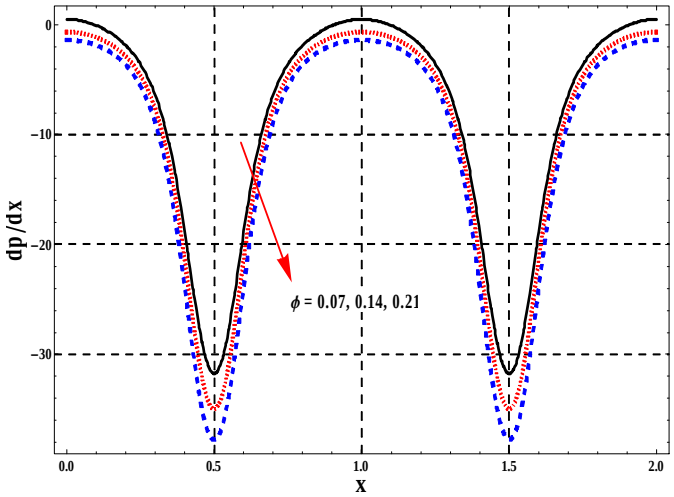

Figure 3.2. Illustration of the dp/dx for different values of CNT's when $\alpha = \frac{\pi}{4}$, $a = 0.7$, $\eta = 0.95$, $Gr = 5.0$, $Br = 0.3$, $\gamma = 0.1$, $\beta = 0.3$ and $\varepsilon = 1.0$.

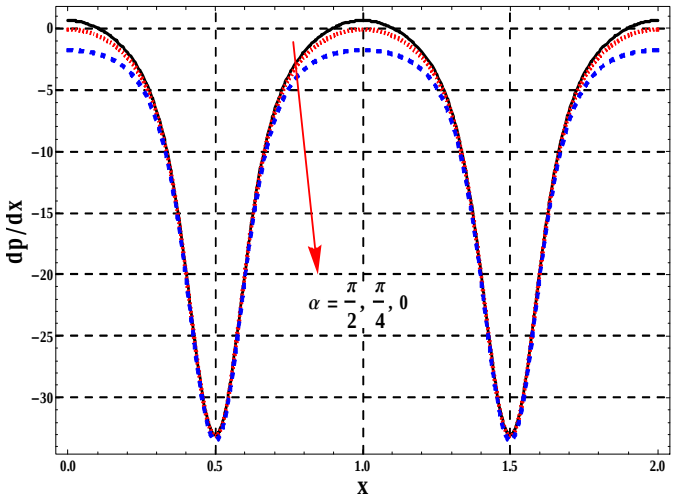

Figure 3.3. Illustration of dp/dx for different α when $\phi = 0.1$, $a = 0.7$, $\eta = 0.95$, $Gr = 5.0$, $Br = 0.3$, $\gamma = 0.1$, $\beta = 0.3$ and $\varepsilon = 1.0$.

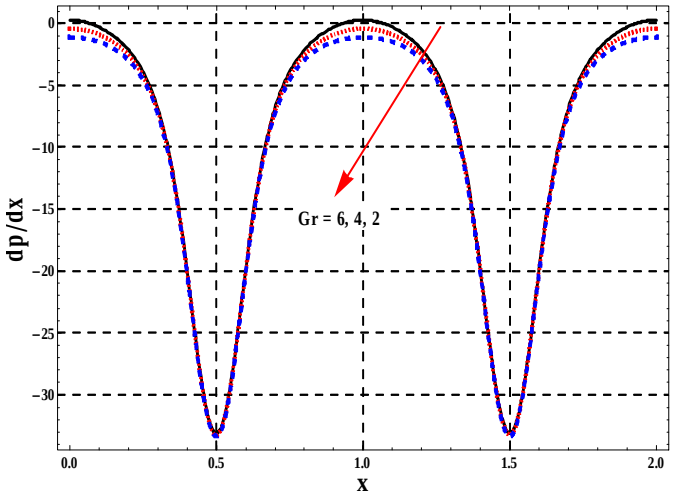

Figure 3.4. Illustration of dp/dx for change in Gr when $\alpha = \frac{\pi}{4}$, $a = 0.7$, $\eta = 0.95$, $\phi = 0.1$, $Br = 0.3$, $\gamma = 0.1$, $\beta = 0.3$ and $\varepsilon = 1.0$.

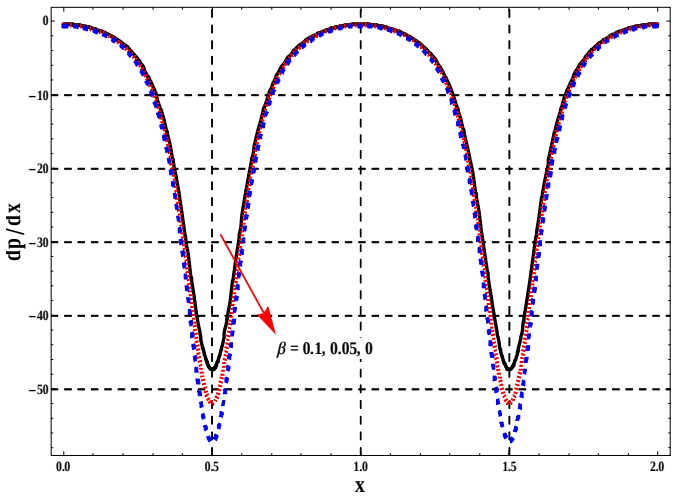

Figure 3.5. Illustration of dp/dx for different values of β when $\alpha = \frac{\pi}{4}$, $a = 0.7$, $\eta = 0.95$, $\phi = 0.1$, $Br = 0.3$, $Gr = 5$, $\gamma = 0.1$, $\phi = 0.1$ and $\varepsilon = 1.0$.

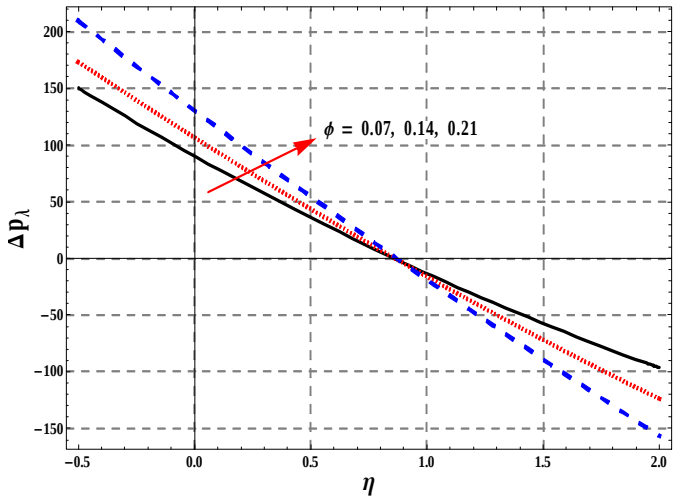

Figure 3.6. Effect of CNT's on Δp_λ when $\alpha = \frac{\pi}{4}$, $a = 0.7$, $Gr = 5.0$, $Br = 0.3$, $\gamma = 0.1$, $\beta = 0.3$ and $\varepsilon = 1.0$.

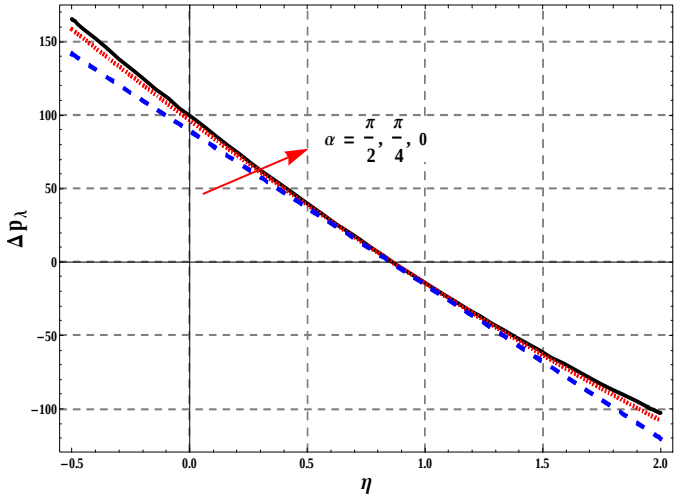

Figure 3.7. Effect of α on Δp_λ when $\phi = 0.1$, $a = 0.7$, $\eta = 0.95$, $Gr = 5.0$, $Br = 0.3$, $\gamma = 0.1$, $\beta = 0.3$ and $\varepsilon = 1.0$.

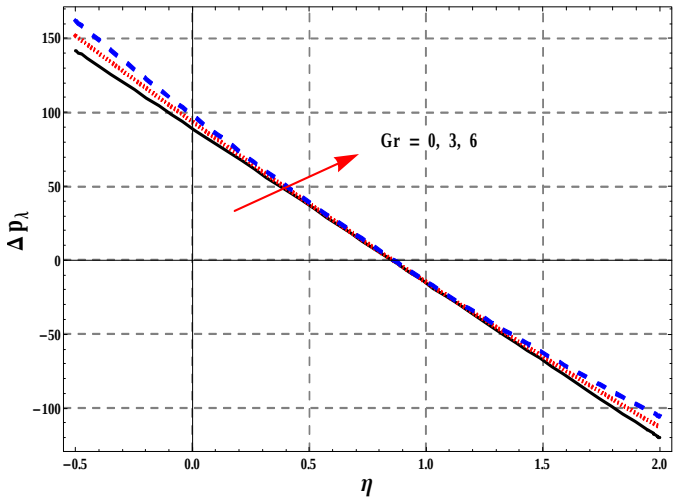

Figure 3.8. Effect of Gr on Δp_λ when $\alpha = \frac{\pi}{4}$, $a = 0.7$, $\phi = 0.1$, $Br = 0.3$, $\gamma = 0.1$, $\beta = 0.3$ and $\varepsilon = 1.0$.

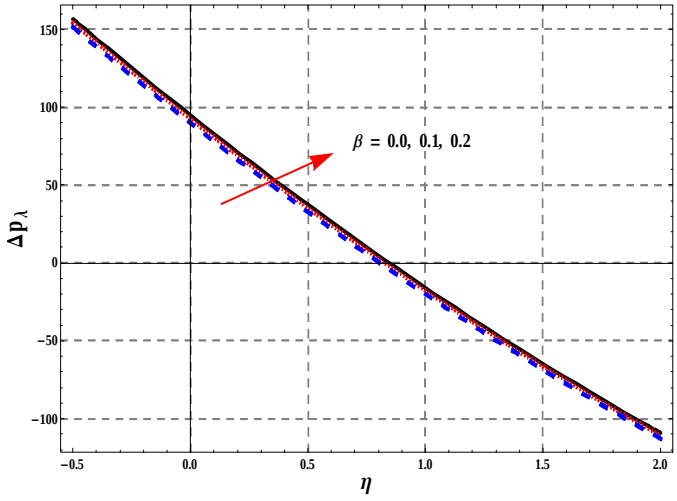

Figure 3.9. Effect of β on Δp_λ when $\alpha = \frac{\pi}{4}$, $a = 0.7$, $\phi = 0.1$, $Br = 0.3$, $\gamma = 0.1$, $\phi = 0.1$ and $\varepsilon = 1.0$.

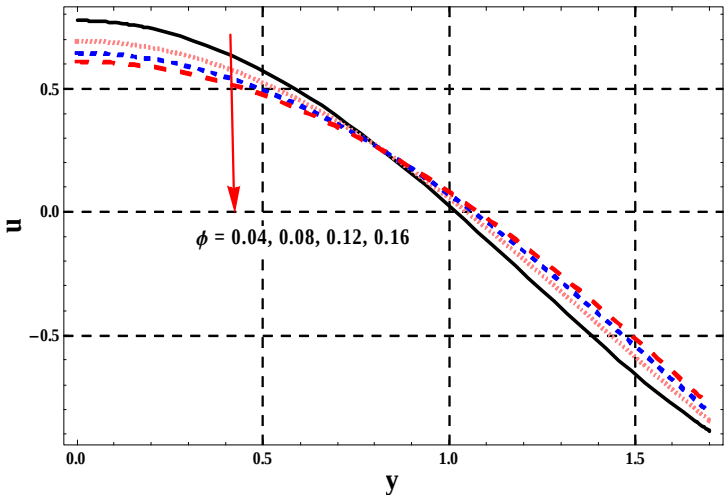

Figure 3.10. Variation in u for distinct values of CNT's when $\alpha = \frac{\pi}{4}$, $a = 0.7$, $\eta = 1.2, x = 1.0$, $Gr = 5.0$, $Br = 0.3$, $\gamma = 0.1$, $\beta = 0.1$ and $\varepsilon = 1.0$.

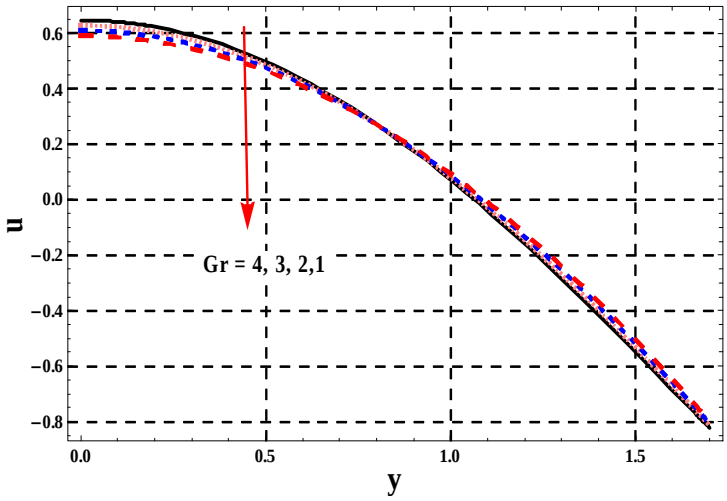

Figure 3.11. Effects of Gr on u when $\alpha = \frac{\pi}{4}$, $a = 0.7$, $\eta = 1.2$, $\phi = 0.1$, $Br = 0.3$, $\gamma = 0.1$, $\beta = 0.1$ and $\varepsilon = 1.0$.

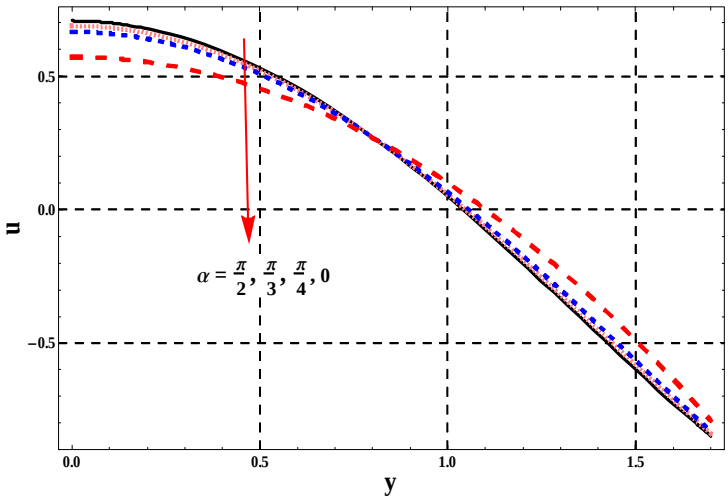

Figure 3.12. Effects of α on u when $\phi = 0.1$, $a = 0.7$, $\eta = 1.2$, $x = 1.0$, $Gr = 5.0$, $Br = 0.3$, $\gamma = 0.1$, $\beta = 0.1$ and $\varepsilon = 1.0$.

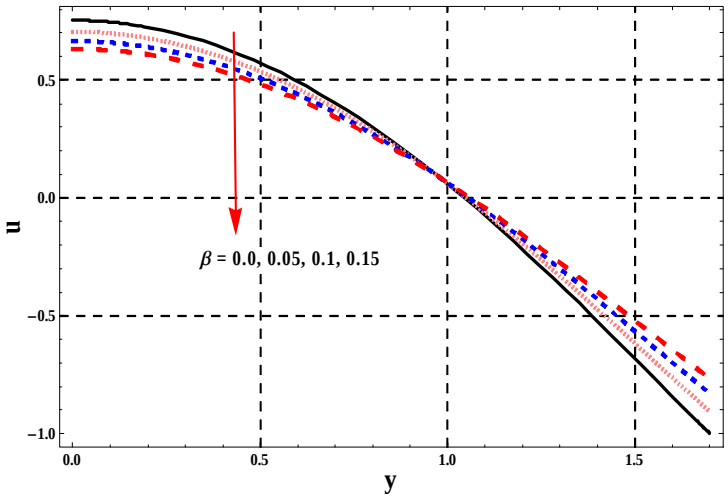

Figure 3.13. Variation in u for distinct values of β when $\alpha = \frac{\pi}{4}$, $a = 0.7$, $\eta = 1.2$, $x = 1.0$, $Gr = 5.0$, $\phi = 0.1$, $Br = 0.3$, $\gamma = 0.1$, $\phi = 0.1$ and $\varepsilon = 1.0$.

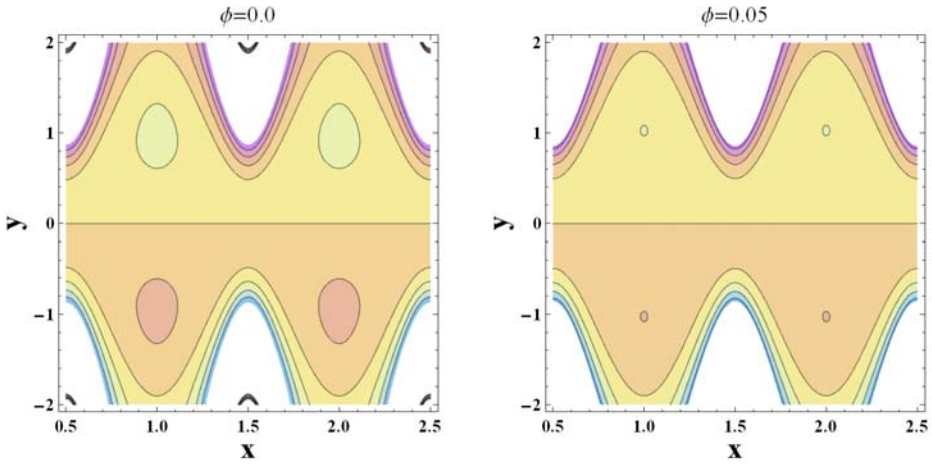

Figure 3.14. Illustration of stream lines when $\alpha = \frac{\pi}{4}$, $a = 0.7$, $\eta = 1.2$, $Gr = 5.0$, $Br = 0.3$, $\gamma = 0.1$, $\beta = 0.3$ and $\varepsilon = 1.0$.

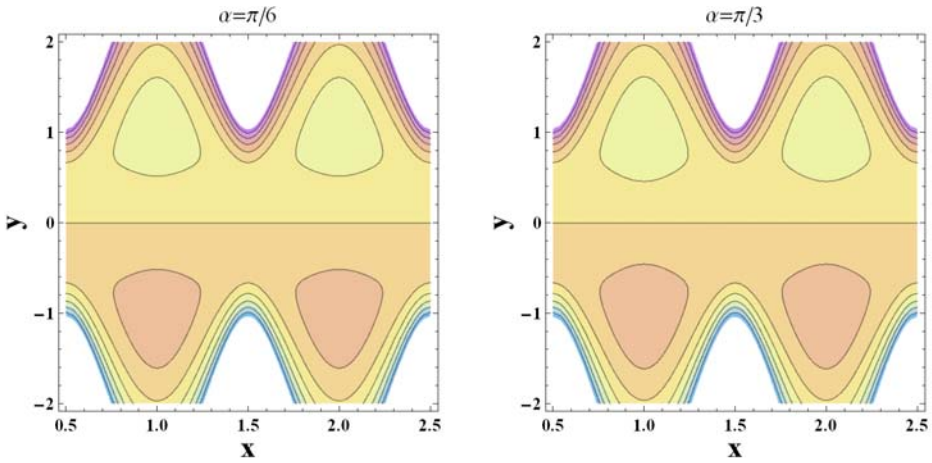

Figure 3.15. Illustration of stream lines when $\phi = 0.1$, $a = 0.7$, $\eta = 1.2$, $Gr = 5.0$, $Br = 0.3$, $\gamma = 0.1$, $\beta = 0.3$ and $\varepsilon = 1.0$.

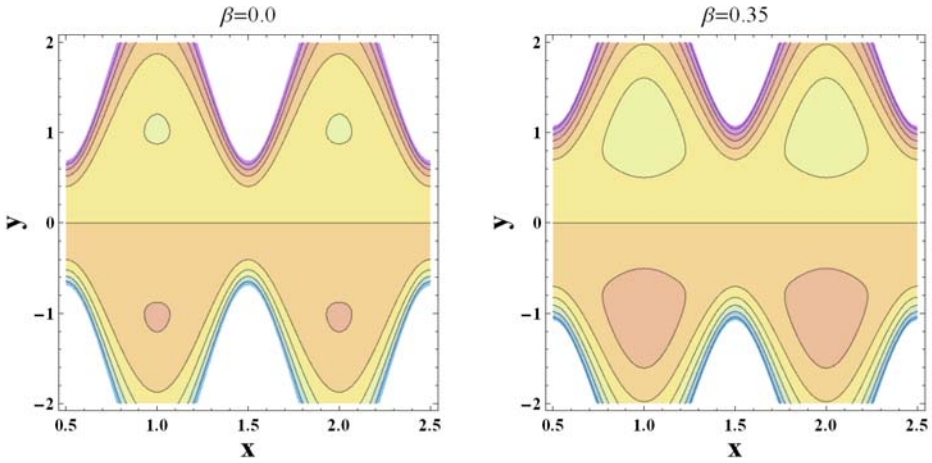

Figure 3.16. Illustration of stream lines when $\alpha = \frac{\pi}{4}$, $a = 0.7$, $\eta = 1.2$, $Gr = 5.0$, $\phi = 0.1$, $Br = 0.3$, $\gamma = 0.1$, $\beta = 0.3$ and $\varepsilon = 1.0$.

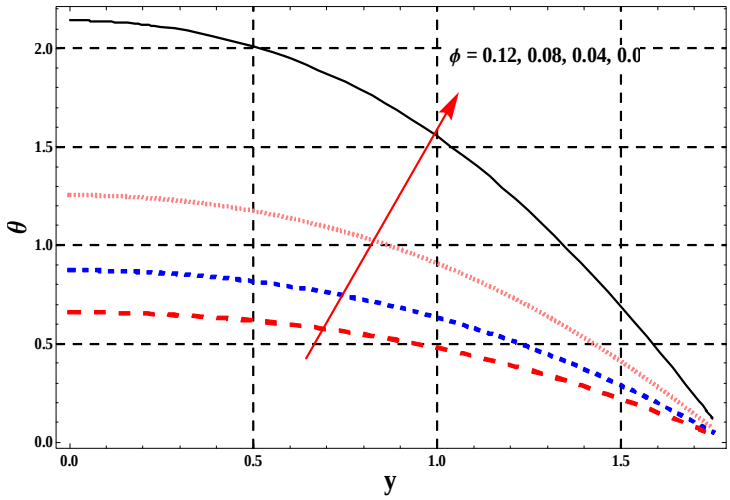

Figure 3.17. Effect of CNT's on θ when $\alpha = \frac{\pi}{4}$, $a = 0.7$, $\eta = 1.2$, $x = 0.1$, $Gr = 5.0$, $Br = 0.3$, $\gamma = 0.1$, $\beta = 0.1$ and $\varepsilon = 1.0$.

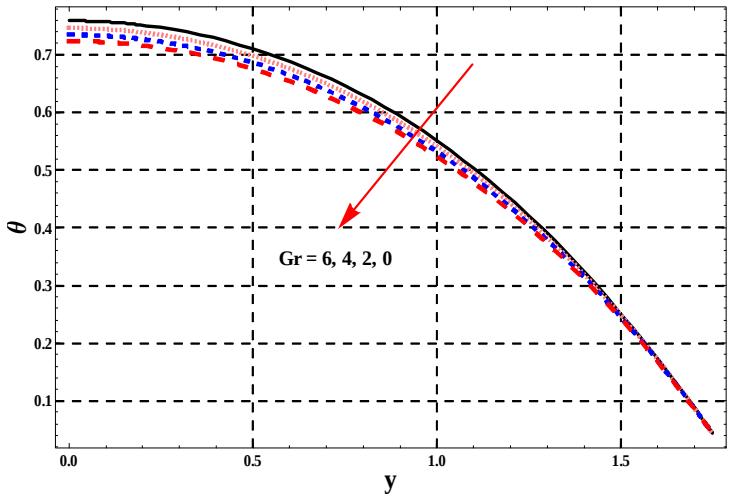

Figure 3.18. Effect of Gr on θ when $\alpha = \frac{\pi}{4}$, $a = 0.7$, $\eta = 1.2$, $x = 1.0$, $\phi = 0.1$, $Br = 0.3$, $\gamma = 0.1$, $\beta = 0.1$ and $\varepsilon = 1.0$.

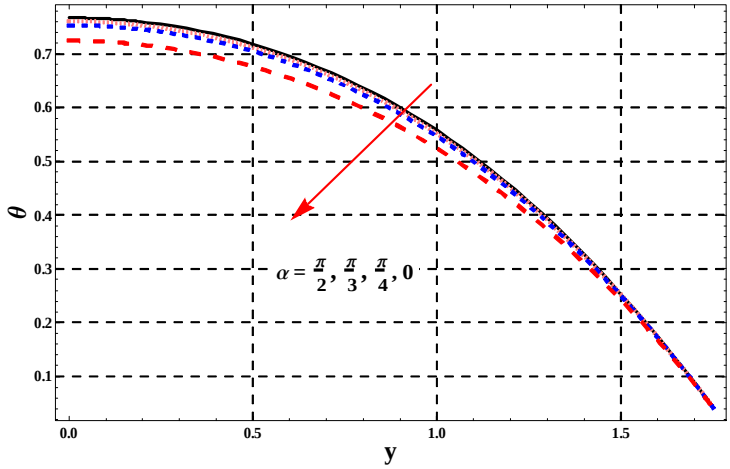

Figure 3.19. Effect of α on θ when $\phi = 0.1$, $a = 0.7$, $\eta = 1.2$, $x = 1.0$, $Gr = 5.0$, $Br = 0.3$, $\gamma = 0.1$, $\beta = 0.1$ and $\varepsilon = 1.0$.

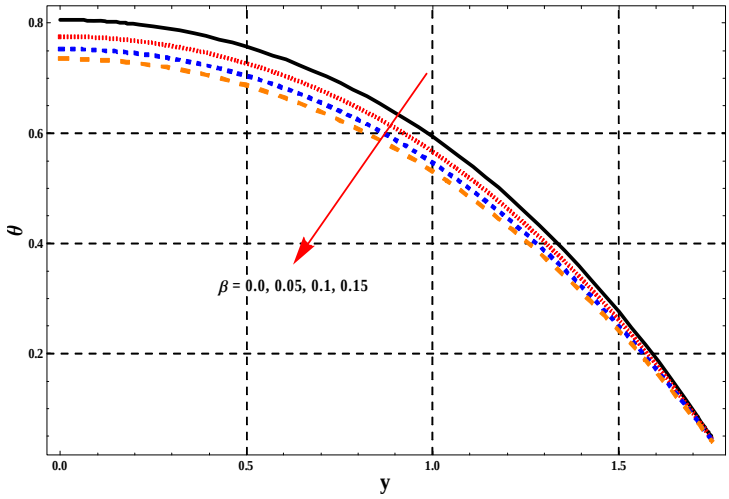

Figure 3.20. Effect of β on θ when $\alpha = \frac{\pi}{4}$, $a = 0.7$, $\eta = 1.2$, $\phi = 0.1$, $x = 1.0, Gr = 5.0$, $Br = 0.3$, $\gamma = 0.1$ and $\varepsilon = 1.0$.

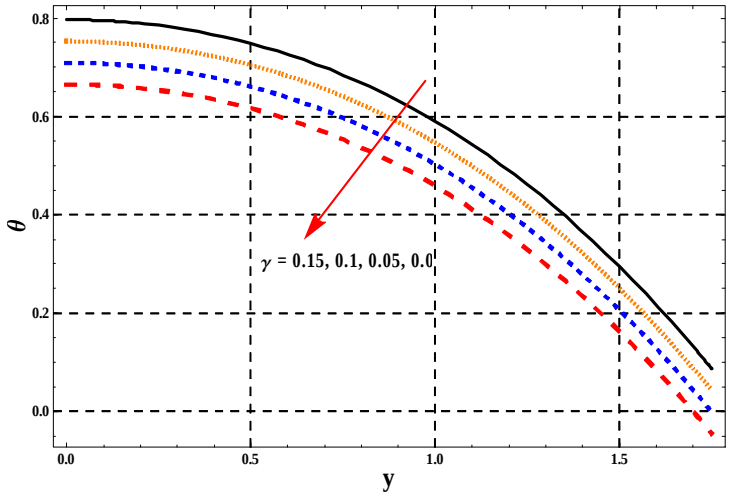

Figure 3.21. Consequence of γ on θ when $\alpha = \frac{\pi}{4}$, $a = 0.7$, $\eta = 1.2$, $x = 1.0, Gr = 5.0$, $\phi = 0.1$, $Br = 0.3$, $\beta = 0.1$ and $\varepsilon = 1.0$.

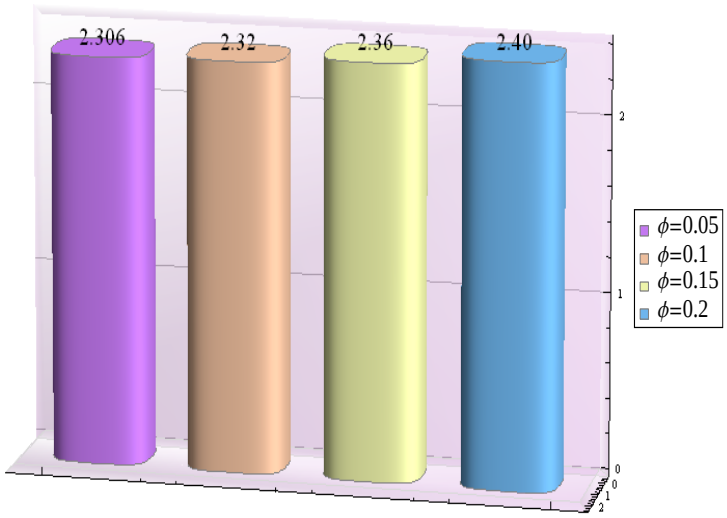

Figure 3.22. Heat transfer rate at the wall for different values of CNT's when $\alpha = \frac{\pi}{4}$, $a = 0.7$, $\eta = 1.2$, $x = 1.0, Gr = 5.0$, $Br = 0.3$, $\gamma = 0.1$, $\beta = 0.1$ and $\varepsilon = 1.0$.

ϕ	Maxwell Model	H-C Model	Xue's Model
0.02	0.917841	0.897584	0.846393
0.04	0.878064	0.845563	0.776018
0.06	0.842368	0.802800	0.728278
0.08	0.810117	0.766884	0.693330
0.1	0.780784	0.736145	0.666257
0.12	0.753928	0.709386	0.644321
0.14	0.729177	0.685725	0.625872
0.16	0.706213	0.664495	0.609852
0.18	0.684763	0.645181	0.595546
0.2	0.66459	0.627377	0.582454

Table 3.2: Statistical data of the axial velocity at the center of channel for different values of nanoparticle volume fraction.

ϕ	H-C Model	Maxwells Model	Xue's Model
0.02	1.88122	2.00445	1.58737
0.04	1.67219	1.88041	1.25446
0.06	1.50084	1.76804	1.03207
0.08	1.35769	1.66566	0.872766
0.10	1.23619	1.57193	0.752911
0.12	1.13170	1.48570	0.659386
0.14	1.04079	1.40604	0.584319
0.16	0.96091	1.33213	0.522694
0.18	0.89010	1.26332	0.471161
0.20	0.82685	1.19900	0.427397

Table 3.3: Statistical data of the temperature at the center of channel for distinct values of nanoparticle volume fraction.

ϕ	H-C Model	Maxwells Model	Xue's Model
0.02	2.37715	2.36294	2.32826
0.04	2.37825	2.35544	2.30946
0.06	2.38242	2.35448	2.30579
0.08	2.38924	2.35837	2.31030
0.10	2.39833	2.36594	2.31977
0.12	2.40942	2.37638	2.33252
0.14	2.42223	2.38912	2.34759
0.16	2.43654	2.40371	2.36440
0.18	2.45214	2.41980	2.38254
0.20	2.46883	2.43712	2.40171

Table 3.4: Statistical data of the heat transfer rate at the wall for different values of nanoparticle volume fraction.

3.8 Concluding remarks

Peristalsis of the SWCNTs is studied here using the three prominent thermal conductivity models. This study concludes that the pressure gradient decreases with an increase of SWCNTs volume fraction while it enhances for larger channel inclination angle, the Grashoff number and the velocity slip parameter. Increase in the values of SWCNTs volume fraction shows an increase of the pressure rise per wavelength in retrograde pumping. It is noted that the axial velocity is decreasing function of SWCNTs volume fraction and velocity slip parameter. The size of trapped bolus decreases with an increase in the SWCNTs volume fraction. Maximum velocity and the temperature channel center are smaller for the SWCNTs when compared with the values obtained for the Cu nanoparticles. Further the heat transfer rate at the boundary for the fluid composed of SWCNTs is small when compared with the fluid composed of Cu nanoparticles.

Bibliography

[1] T. W. Latham, Fluid motion in a peristaltic pump, MS Thesies, MIT Cambridge, MA, 1996.

[2] M. Y. Jaffrin and A. H. Shapiro, Peristaltic pumping, Ann. Rev. Fluid Mech. 3 (1971) 13-16.

[3] Y. C. Fung and C. S. Yih, Peristaltic transport, Trans. ASME J. Appl. Mech. 33 (1968) 669-675.

[4] L. M. Srivastava and V. P. Srivastava, Peristaltic transport of blood: Casson model-II, J. Biomech. 17 (1984) 821-830.

[5] T. Hayat, N. Alvi and N. Ali, Peristaltic mechanism of a Maxwell fluid in an asymmetric channel, Nonlinear Anal. Real Word Appl. 9 (2008) 1474-1490.

[6] N. Ali, M. Sajid and T. Hayat, Long wavelength flow analysis in a curved chanel, Zeitschrift fur Naturforschung A 65a (2010) 191-196.

[7] S.U.S. Choi, Enhancing thermal conductivity of fluids with nanoparticles. ASME Fluids Eng. Div. 231 (1995) 99-105.

[8] S. Dong, L. Zheng, X. Zhang and P. Lin, Improved drag force model and its application in simulating nanofluid flow, Microfluid Nanofluid 17 (2014) 253-261.

[9] K. Khanafer, K. Vafai and M. Lightstone, Buoyancy-driven heat transfer enhancement in a two dimensional enclosure utilizing nanofluids. Int. J. Heat Mass Transfer, 46 (2003) 3639-3653.

[10] S. A. Shehzad, F. M. Abbasi, T. Hayat, Faud Alsaadi, Model and comparative study for peristaltic transport of water based nanofluids. Jornal of Molecular Liquids, 209 (2015) 723-728.

[11] Y. Xuan, Q. Li, Investigation on convective heat transfer and flow features of nanofluids. ASME J. Heat transfer, 125 (2003) 151-155.

[12] HC. Brinkman, The viscosity of concentrated suspensions and solutions. J. Chem. Phys. 20 (1952) 571-581.

[13] J. Buongiorno, Convective transport in nanofluids. ASME J. Heat Transfer, 128 (2006) 240-250.

[14] M. Turkyilmazoglu, Exact analytical solutions for heat and mass transfer of MHD slip flow in nanofluids. Chemical Engineering Science, 84 (2012) 182-187.

[15] M. Turkyilmazoglu, Nanofluid flow and heat transfer due to a rotating disk. Comput. Fluids 94 (2014) 139-146.

[16] M. Sheikholeslami, M. Gorji-Bandpy, D. D. Ganji and S. Soleimani, Heat flux boundary condition for nanofluid filled enclosure in presence of magnetic field. J. Mol. Liq. 193 (2014) 174-184.

[17] B. H. Thang, P. H. Khoi and P. N. Minh, A modified model for thermal conductivity of carbon nanotube-nanofluids. Physics Fluids, 27 (2015) 032002.

[18] R. Ul Haq, S. Nadeem, Z.H. Khan and N.F.M. Noor, Convective heat transfer in MHD slip flow over a stretching surface in the presence of carbon nanotubes. Physica B: Condensed Matter, 457 (2015) 40-47.

[19] F. M. Abbasi, T. Hayat. B. Ahmad and G. Q. Chen, Slip effects on mixed convective peristaltic transport of copper-water nanofluid in an inclined channel. PLoS One, 9(8) (2014) e105440.

[20] S. A. Shehzad, F. M. Abbasi, T. Hayat and F. Alsaadi, MHD mixed convective peristaltic motion of nanofluid with Joule heating and thermophoresis effects. PLoS One, 9(11) (2014) e111417.

[21] F. M. Abbasi, T. Hayat and B. Ahmad, Impact of magnetic field on mixed convective peristaltic flow of water based nanofluids with Joule heating. Z. Naturforsch 70a (2015) 125–132.

[22] J.C. Maxwell, A treatise on electricity and magnetism. 2nd Edition Oxford University press, Cambridge, 1904, 435-441.

[23] R.L. Hamilton and O.K. Crosser, Thermal conductivity of heterogeneous two component systems. EC Fundam. 1 (1962) 187-191.

[24] Q.Z. Xue, Model for thermal conductivity of carbon nanotube-based composites. Physica B 368 (2005) 302-307.

[25] M. Jafari, M. Farhadi and K. sedighi, Single walled carbon nanotube effects on mixed convection heat transfer in an Enclosure: a LBM approach. TPNMS 2 (2014) 14-28.